SciMedCentral

JSM Clinical Pharmaceutics

Original Article

Design, Synthesis and Biological Evaluation of Hybrid C3-Quinazolinone linked β-carboline Conjugates as DNA Intercalative Topoisomerase I Inhibitors

Yellaiah Tangella[1,2], Manda Sathish[1,3], Manasa Kadagathur[4], Narayana Nagesh[5]* and Bathini Nagendra Babu[1,2]*

[1]*Fluoro-Argochemicals, CSIR-Indian Institute of Chemical Technology, Hyderabad-500 007, India*

[2]*Academy of Scientific and Innovative Research, New Delhi 110025, India*

[3]*Centro de Investigación de Estudios Avanzados del Maule, Vicerrectoría de Investigación y Posgrado, Universidad Católica del Maule, Talc 3466706, Chile*

[4]*Department of Medicinal Chemistry, National Institute of Pharmaceutical Education and Research, Hyderabad-500 037, India*

[5]*Medical Biotechnology Complex, ANNEXE-II, CSIR-Centre for Cellular and Molecular Biology, Uppal Road, Hyderabad 500007, India*

***Corresponding author**

Dr. Narayana Nagesh, Medical Biotechnology Complex, ANNEXE-II, CSIR-Centre for Cellular and Molecular Biology, Uppal Road, Hyderabad 500007, India; Fax: +91-40-27160310, +91-40- 27195563, Email: nagesh@ccmb.res.in

Submitted: 13 August 2021

Accepted: 31 August 2021

Published: 04 September 2021

ISSN: 2379-9498

Keywords

- Anticancer
- β-carbolines
- Quinazolinones
- DNA
- Topoisomerase

Abstract

In the present study, a series of new C3-quinazolinone linked β-carboline conjugates were synthesized successfully and evaluated as DNA intercalative topo I inhibitors. It was found that most of the compounds showed good cytotoxic activity, in particular, compounds 10a, 10e and 10u are exhibited potent cytotoxicity against all the tested four cell lines with IC50 values are ranging from 1.19±0.33 to 5.37±0.28 μM. topo I mediated DNA relaxation assay results showed that these compounds could significantly inhibit the activity of topo I. The structure-activity relationship studies indicate the importance of the substitutions at C1 and C3 positions of the β-carboline moiety. These compounds induced cell cycle arrest in G2/M phase. Further, spectroscopic studies substantiated the biological activities as well as the nature of interactions with the DNA. The intercalative mode of binding with the DNA was established by several biophysical studies like UV- visible, fluorescence and circular dichroism and viscosity. The results obtained from biophysical studies were further supported by the molecular docking studies.

ABBREVATIONS

Topo I: Topoisomerase I; **DNA:** Deoxyribonucleic acid; **UV:** Ultraviolet; **CDK:** Cyclin- dependent kinases; **MK:** Myokinase; **IKK:** IκB kinas; **PKL1**: Polo-like kinase 1; **$SOCl_2$:** Thionyl chloride; **MeOH:** Methanol; **EtOH:** Ethanol; **TCCA:** Trichloroisocyanuric acid; **Et3N**: Triethylamine; **DMF:** Dimethylformamide; **NaOH:** Sodium hydroxide; **DCM:** Dichloromethane; **EDCI.HCl:** 1-(3-Dimethylaminopropyl)-3-ethylcarbodiimide hydrochloride; **HOBt:** Hydroxybenzotriazole; **AC_2O:** Acetic anhydride; **Fe:** Iron; NH_4Cl: Ammonium chloride; **AcOH:** Acetic acid.

INTRODUCTION

Cancer is one of the major health burdens to the society and millions of new cases are expecting in near future. Most of the cancers are recognized by un-inhibited growth of cells without differentiation due to de-regulation of proteins and critical enzymes, which controls cell division and proliferation(1). Although much development has been made from the early detection methods to treat cancer, the factors like drug resistance, drug- induced toxicities, target specificity and poor patient compliance are strongly inducing the discovery of new potent cancer chemotherapeutics with improved pharmacological properties along with specific target(2). Nowadays, the discovery of new hybrid molecules which can recognize DNA and exhibit anticancer activity has emerged as a significant research area in drug discovery (3) . The DNA binding agents are mainly categorized into three types based on their mode of interaction, such as i) groove binders ii) intercalators and iii) combilexins. This type of drugs exhibits anticancer activity through their significant interactions with double helix DNA or associated enzymes by forming hydrogen bonds and/or stable complexes leading to conformational changes,

which affect the usual mechanisms of DNA(4). Especially, DNA topoisomerases regulates the topological changes between two DNA strands during transcription and replication, and thus are significant and ubiquitous enzymes required for cell growth and proliferation. The enzymes which cleave and reseal one strand of DNA are defined as topoisomerase I (topo I) enzymes whereas topos that cleave and reseal both strands to generate staggered double-strand breaks are defined as topoisomerase II (topo II) enzymes(5). Until recently, very few topo I inhibitors were known, for instance camptothecin (CPT) and its derivatives(6). harmine (Figure 1) and its derivatives, and norharmane (7). By considering these facts, the pursuit towards the design and development of novel hybrid molecules that could target topo I holds an attractive tool for discovery of new anticancer agents. Natural products are playing a vital role in drug discovery, due to their exceptional achievements to fight against many life threatening diseases. Moreover, majority of the anticancer drugs currently in clinical use are either natural products or derived from their scaffolds. Among them, β-carboline are an important class of natural and synthetic iodole alkaloids due to their intrinsic biochemical effects and pharmacological properties (8). The recent literature on β-carbolines revealed that these are exhibiting cytotoxic activity through various mechanisms of action such as inhibiting topo I and topo II,(9) intercalating with DNA,(10)DNA groove binders,11 MK- (2,12) CDK, (13) kinesin Eg (5,14) IKK (15) and PLK1.(16) Apart from, some of these compounds are also showing anti- cancer activity through a photocleavage of DNA and histone deacetylase (HDAC) inhibitor. (9,17) Most of the DNA targeting anticancer agents/drugs shows their efficacy by recognition and binding to DNA through intercalation via G-C base pairs, such examples are Mana-Hox (Figure 1), dactinomycin and doxorubicin.10b Some other literature reports demonstrated that β-carbolines containing a substituted phenyl group at the C1 position and certain biologically significant heterocyclic scaffolds like 1,2-pyrazoles, 1,2,4- triazole, 1,3,4-oxadiazole, 4-benzylidene-4*H*-oxazol-5-one, or a functionalized carbohydrazide moiety at the C3 position allow them to exhibit potent cytotoxicity. (18) The structure–activity relationship (SAR) studies open that the introduction of suitable substituents at the C1 and C3 positions of the β-carboline core accentuated antitumor activity and DNA binding ability. On the other hand, the quinazoline is a benzene-fused pyrimidine derivative, which is often appearing in a variety of biologically active natural products and synthetic compounds.19 For instance, gefitinib and erlotinib are well known anticancer drugs possess this ring structure.20 Due to its structural resemblance to purine, pteridine and pyrimidine, quinazoline has frequently been employed as a bioisosteric replacement for these biologically important heterocycles in molecular design. The quinazolinone scaffold has abundant existence in wide variety of natural products (21) and has attracted immense interest in the past few decades due to the promising bio-activity of its derivatives ranging from antimicrobial, antimalarial, anti-inflammatory, antihypertensive, antidiabetic and anticonvulsant, to antitumor activities (Figure 1). (22) Some of these derivatives are acting as a ligands for AMPA and benzodiazepine receptors in the CNS system or as DNA binders. (23) Moreover, 2-methyl quinazolinone derivatives are acting as inhibitors of DNA repair enzyme poly (ADP-ribose) polymerase (PARP). (24) Cytotoxic activity is frequently found property in several members of quinazolinones derivatives. In particular, 2,3-disubstituted-4(3H)-quinazolinones have gained commercial relevance in the form of drugs such as rutaecarpine (anti-inflammatory activity), afloqualone (sedative activity), (+)-febrifugine (antimalarial activity) and (–)-chaetominine (anticancer activity). (25) (–)-Chaetominine is a tripeptide alkaloid that displaying stronger cytotoxic activity than 5-fluorouracil against human colon cancer SW1116 and leukemia K562 cell lines.(25) In recent years, combination chemotherapy, a single drug molecule containing more than one pharmacophores that simultaneously interact with multiple drug targets has emerged as a significant tool in drug discovery for the treatment of cancer. (26) This approach aims to diminish issues that are commonly associated with single-target drugs like limited efficacies and development of resistance. (27) In view of the therapeutic significance of β- carbolines and 2,3-disubstituted quinazolinones and to study the influence of the substituents at C1 and C3 position of the β-carboline scaffold in depth, as well as our interest in developing novel

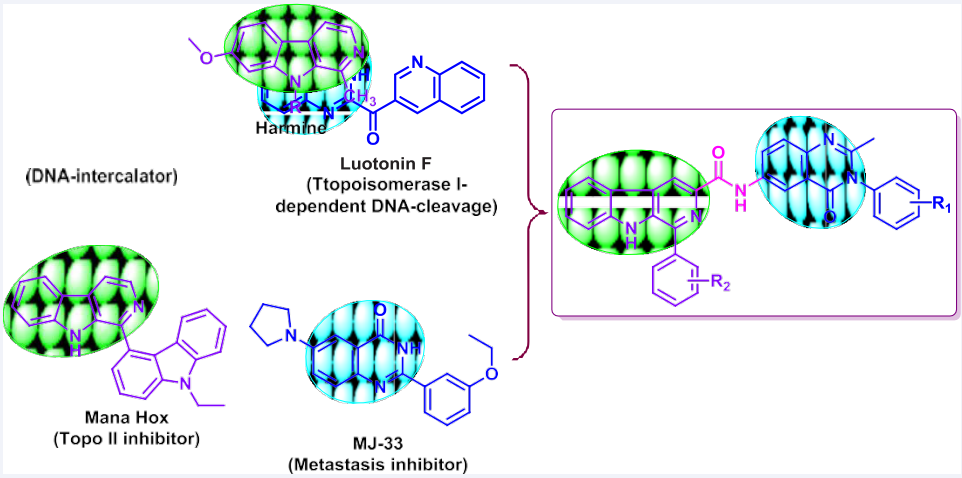

Figure 1 Pharmaceutically important β-carboline and quinazolinone derivatives and rational design strategy of β-carboline-quinazolinone conjugates.

hybrid molecules as potential anticancer agents, we designed and synthesized a series of new hybrid compounds (Figure 1). In these hybrid compounds, the β-carboline and quinazolinone pharmacophores were connected via amide bond. Herein, we report the preparation, cytotoxicity and DNA binding properties of C3 quinazolinone linked β-carboline conjugates. The main focus of the present investigation is to evaluate the effect of these compounds on DNA, by examining topo I inhibition, DNA binding, conformation and viscosity studies. The possible ways in which these compounds might interact with DNA was also elucidated by molecular docking studies.

RESULTS AND DISCUSSION

Chemistry

Synthetic protocols followed for the synthesis of new quinazolinones linked β-carboline conjugates from commercially available starting materials are outlined in Schemes 1 an As shown in Scheme 1, 2-amino-5-nitrobenzoic acid (1) was converted into 2-methyl- 6-nitro-4*H*- benzo (D) 1,3 oxazin -4-one (2) by refluxing in acetic anhydride. Subsequently, the functionalize quinazolin-4-one core was generated by a ring-opening and ring-closure reaction with variously substituted anilines under reflux in acetic acid. Finally, an iron-mediated reduction of nitro group by refluxing in acidic condition yielded the desired fragment amino substituted quinazolinones (4a-g.) Later, the synthetic route for these final hybrid compounds is depicted in (Scheme 2). The first synthetic step involved the esterification of L-tryptophan (5) by using $SOCl_2$ to afford the desired L- tryptophan methyl ester hydrochloride **(6)**. Then condensation of 6 with various substituted benzaldehydes under reflux provides the corresponding tetrahydro-β- carboline esters **7a-e** through a well-known Pictet–Spengler reaction, which were further oxidized without purification to get fully aromatized **β**-carboline esters (8a-e) by using TCCA (Trichloroisocyanuric acid) at room temperature. The ester functionality at a C3 position of 8a-e was then hydrolyzed to its corresponding β-carboline acids (9a-e) by using NaOH. Finally, the desired quinazolinones linked β-carboline conjugates 10a-z, 10aa and 10ab were obtained in excellent yields by an acid-amine coupling reaction using 1-ethyl-3-(3- dimethylaminopropyl)carbodiimide (EDC) and hydroxybenzotriazole (HOBt). The structures of all synthesized compounds 10a-z, 10aa and 10ab,(table 1) were confirmed by high resolution mass spectrometry, ^{1}H and ^{13}C NMR spectroscopy.

Biological studies

Cytotoxicity: To evaluate the cytotoxic potential of synthesized β-carboline conjugates, we performed the MTT assay against a panel of four human cancer cell lines such as A549 (lung cancer), MCF-7 (breast cancer), DU-145 (prostate cancer), HeLa (cervical cancer) and normal cells i.e. NIH3T3 (mouse embryonic fibroblast cells). MTT assay was done thrice and the mean values were shown in below. The results of this cytotoxic data are expressed as IC_{50} values in micro molar (μM) and are depicted in (Table 2). To get more meaningful comparisons of relative potencies harmine and doxorubicin were employed as positive controls. The screening results revealed that these β-carboline conjugates exhibited good cytotoxic activities against tested cancer cells (IC_{50} values ranging from 01.19±0.33 to 47.50±3.23

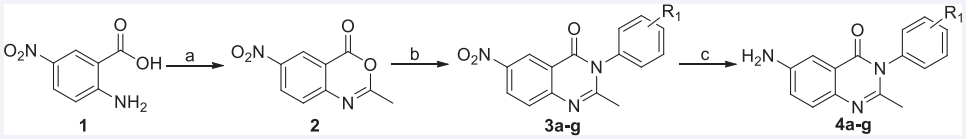

Scheme 1 Reagents and conditions: (a) AC_2O, 150 °C, 1 h, 90%; (b) Anilines (**a**: R_1 = 2-OMe, **b**: R_1 = 3-OMe, **c**: R_1 = 4-OMe, **d**: R_1 = 3-Me, **e**: R_1 = 3-Cl, **f**: R_1 = 3-CF_3, **g**: R_1 = 3,4,5-OMe), AcOH, reflux, 5 h, 75-84%; (c) Fe, NH_4Cl, MeOH:H_2O (2:1), 100 °C, 4 h, 82-92%.

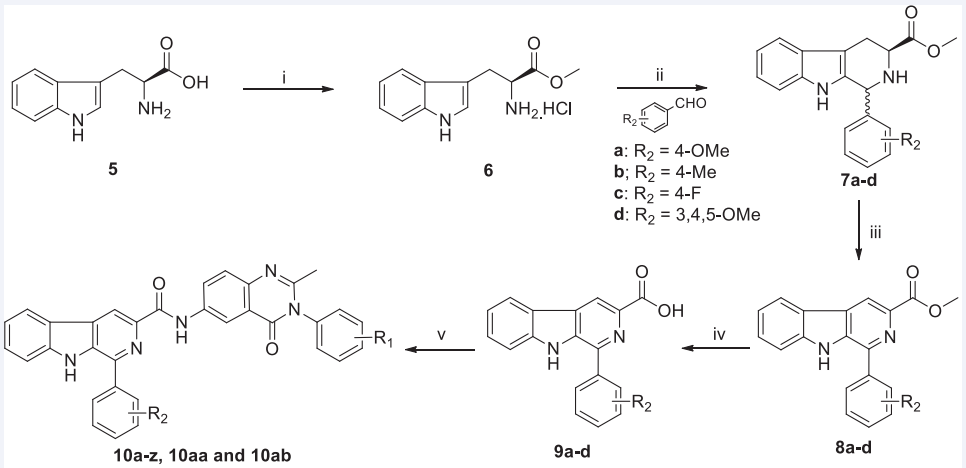

Scheme 2 Reagents and conditions: (i) SOCl2, MeOH, 0 oC-rt, 12 h, 88%; (ii) Benzaldehydes, EtOH, reflux, 12 h, 78-92%; (iii) TCCA, Et3N, DMF, 0 oC-rt, 4 h, 70-86%; (iv) 2N NaOH, MeOH, reflux, 5 h, 81-94%; (v) 5a-g, EDCI.HCl, HOBt, Et3N, DCM, 0 oC-rt, 12 h , 80-93%.

Table 1: Details of substituents attached to the synthesized compounds.

S.No.	Compound	R_1	R_2
1	**10a**	2-OMe	4-OMe
2	**10b**	3-OMe	4-OMe
3	**10c**	4-OMe	4-OMe
4	**10d**	3-Me	4-OMe
5	**10e**	3-Cl	4-OMe
6	**10f**	3-CF_3	4-OMe
7	**10g**	3,4,5-OMe	4-OMe
8	**10h**	2-OMe	4-Me
9	**10i**	3-OMe	4-Me
10	**10j**	4-OMe	4-Me
11	**10k**	3-Me	4-Me
12	**10l**	3-Cl	4-Me
13	**10m**	3-CF_3	4-Me
14	**10n**	3,4,5-OMe	4-Me
15	**10o**	2-OMe	4-F
16	**10p**	3-OMe	4-F
17	**10q**	4-OMe	4-F
18	**10r**	3-Me	4-F
19	**10s**	3-Cl	4-F
20	**10t**	3-CF_3	4-F
21	**10u**	3,4,5-OMe	4-F
22	**10v**	2-OMe	3,4,5-OMe
23	**10w**	3-OMe	3,4,5-OMe
24	**10x**	4-OMe	3,4,5-OMe
25	**10y**	3-Me	3,4,5-OMe
26	**10z**	3-Cl	3,4,5-OMe
27	**10aa**	3-CF_3	3,4,5-OMe
28	**10ab**	3,4,5-OMe	3,4,5-OMe

Table 2: Cytotoxic activity of β-carboline conjugates 10a-z, 10aa and 10ab against a panel of human cancer cell lines (IC50 values in μM).

Compound	A549[b]	DU-145[c]	MCF-7[d]	HCT116[e]	NIH3T3[f]
10a	01.45±0.75	01.71±0.22	03.31±1.33	04.86±0.44	07.64±0.65
10b	02.09±0.23	03.16±1.35	12.22±0.11	13.38±2.19	08.76±2.84
10c	10.50±2.37	16.00±0.44	21.11±0.38	20.58±0.36	25.56±1.24
10d	09.39±0.73	08.44±0.36	14.28±3.55	18.69±0.29	21.74±2.15
10e	01.19±3.33	01.33±3.36	05.37±0.28	03.60±0.47	07.56±0.48
10f	01.32±0.65	02.24±0.66	13.93±0.47	06.35±0.57	15.78±3.44
10g	08.93±0.72	05.25±0.56	17.25±2.56	19.08±1.69	22.76±1.25
10h	14.37±1.46	17.41±1.37	19.86±2.45	35.29±2.28	37.58±3.13
10i	19.83±1.37	26.00±0.77	17.09±0.22	29.19±0.38	32.87±3.84
10j	10.37±0.67	17.40±2.26	23.00±0.28	20.73±1.18	27.97±1.66
10k	02.19±0.73	05.15±0.87	11.00±1.39	18.71±0.22	21.87±2.54
10l	12.88±0.39	15.86±0.46	18.76±0.18	21.90±0.56	25.87±2.57
10m	02.10±3.56	08.77±0.76	12.00±0.11	16.32±0.38	19.27±0.45
10n	13.12±0.82	18.74±1.66	16.63±0.65	17.38±1.86	19.45±2.15
10o	04.59±0.98	12.58±0.83	17.17±2.36	28.88±0.65	32.67±3.48
10p	08.62±0.57	17.70±0.11	22.19±0.33	33.63±0.38	37.54±3.18
10q	01.58±2.83	05.42±0.49	13.70±0.16	13.03±0.28	15.87±0.33
10r	06.81±0.65	09.23±3.65	18.70±0.28	15.39±0.11	21.56±1.56
10s	10.48±1.95	15.74±2.63	20.54±0.29	26.76±3.25	29.45±2.42

10t	09.28±0.72	21.77±0.95	25.95±1.17	28.86±0.14	32.98±1.84
10u	01.42±1.47	01.69±1.59	03.98±0.45	05.28±0.26	07.45±0.82
10v	03.63±0.87	09.73±0.49	10.00±0.38	17.11±0.28	19.87±0.37
10w	13.23±0.22	14.66±0.19	17.94±1.29	19.78±0.37	22.45±3.43
10x	08.54±1.65	12.16±1.02	23.12±2.22	15.10±1.33	25.65±1.47
10y	10.32±2.86	05.64±0.36	12.82±0.11	22.00±0.17	27.34±2.34
10z	08.64±0.22	13.91±2.31	24.47±0.18	23.05±0.22	28.53±1.19
10aa	16.64±2.33	15.17±1.78	30.67±1.16	34.23±1.58	37.65±2.19
10ab	19.26±2.46	20.86±2.38	47.50±3.23	17.88±2.27	49.33±2.74
Doxorubicin	01.26±0.45	01.49±2.21	01.10±0.18	01.91±0.87	01.97±0.22
Harmine	06.05±0.23	10.63±1.14	10.76±1.12	09.76±0.56	11.14±0.24

[a]50% Inhibitory concentration after 48 h of drug treatment. [b]Human lung cancer. [c]Human prostate cancer. [d] Human breast cancer. [e] Human colon cancer.[f] Mouse embryonic fibroblast cells

Table 3: Percentage of panoptic cells observed when A549 cancer cells were treated with 1 and 2 μM concentrations of **10a** and **10e.**

Sample	Sub G1 %	G0/G1 %	S %	G2/M %
A: Control (A549)	09.15 ±1.03	57.01±3.22	13.48±2.11	20.83±2.11
B: **10a** (1 μM)	08.65±1.56	53.14±2.31	17.32±1.35	22.54±2.45
C: 10a (2 μM)	03.66±2.17	16.73±0.93	21.45±2.87	56.48±2.43
D: **10e** (1 μM)	07.61±3.11	55.23±2.28	14.42±2.54	24.24±3.22
E: **10e** (2 μM)	05.24±2.74	15.17±3.16	19.65±1.33	59.29±3.87

μM). It is worthwhile mentioning that most of the compounds shown higher cytotoxicity than one of the positive control harmine, which is known DNA intercalator. Compounds **10a**, **10e** and **10u** exhibited similar cytotoxic potential against A549 and DU-145 like another positive control doxorubicin. Among the series of twenty eight compounds, two of them **10a,10e** displayed significant cytotoxicity ≤5.37±0.28 μM and twenty compounds showed <25 μM against all the examined cell lines. In the present study, these conjugates exhibited higher cytotoxicity (nine compounds <5 μM) against A549 lung cancer cell line compared to other tested cell lines. The most active compounds in the series are 10a, 10e , 10u with IC_{50} values ranging from 01.19±0.33 to 5.37±0.28 μM in the tested cell lines. All the compounds exhibited comparatively lesser cytotoxicity in non-malignant cell line namely mouse embryonic fibroblast cell line (NIH3T3 cell lines). The cytotoxic screening results of these conjugates allow a rudimentary picture of the structure-activity relationship (SAR) studies. It was observed that the cytotoxic activity of these 1,3-disubstituted β-carboline conjugates depends on the nature as well as position of the substituents present on both the phenyl rings (R_1 and R_2) of β-carboline and quinazolinone scaffold. The cytotoxic results manifested that the different substituted groups to the C1-phenyl ring (R_2) follow this trend: 4-OMe>4-F>4-Me>3,4,5-OMe. Furthermore, it was noticed that the substituents present at the 2nd and 3rd position of C3-linked quinazolinone moiety (R_1) displayed significant cytotoxic activity irrespective of the electronic nature of the substituents. Among the series, compounds **10a**, **10e**, and **10u** were showed potent cytotoxicity compared to other compounds, which possess 4- OMe and 4-F substituents at the C1-phenyl and 2-OMe, 3-Cl, and 3,4,5-OMe at the C3- linked quinazolinone scaffold. Compounds (10o-v) with Fluoro substitution on the phenyl ring of β-carboline moiety (R_2) have displayed prominent activity, possibly due to lipophilic nature of fluorine. Moreover, compounds with a 2-OMe at R_1 10a, 10h, 10o, and 10v showed considerable cytotoxicity compared to the other compounds with various functional groups at different positions. It is worthwhile to note that, compounds with 3,4,5-OMe groups at R_2 10v-10ab are the weakest cytotoxic members of the series, probably due to the steric factor or may be the effect of a different binding configuration for individual compounds to their cellular targets. SAR studies revealed that mostly the electron-donating substituents (OMe and Me) present on both phenyl rings (R_1 and R_2) of quinazolinone and β-carboline represent the most optimal structures for this class of compounds that display remarkable cytotoxic activity. Based on the MTT assay screening results, the most active compounds 10a, 10e and 10u were further investigated for detailed biological studies, such as DNA topoisomerase I inhibition and cell cycle analysis. In addition, DNA binding spectroscopic, viscosity and molecular docking studies were also performed to ascertain the DNA binding nature of these compounds.

Cell cycle analysis: Most of the anticancer agents exert their growth inhibitory effect either by induction of apoptosis or by arresting the cell cycle at a particular checkpoint or a combination of both. (28) The MTT assay screening results revealed that the test compounds **10a, 10e** induced the significant inhibition of human lung cancer cells (A549) with IC50 values 1.44 and 1.41 μM respectively. A cell cycle analysis was performed thrice to examine the cell cycle alterations induced by these compounds in A549 cancer cell line to understand the phase distribution. Therefore, cancer cells were treated with these active compounds at two concentrations of 1 and 2 μM respectively for 48 h, and the obtained results clearly indicated that these compounds exhibited cell cycle arrest in G2/M phase in comparison with the

untreated control cells. In untreated A549 cells, 20.83%±2.11 of cells were observed in G2/M phase. The cell cycle arrest in G2/M phase is a common cellular response to numerous DNA damaging agents. On treating A549 cells with 1 μM of **10a** and **10e**, the cells exhibited 22.54±2.45 % and 24.24±3.22 % respective cell cycle inhibition in G2/M phase. By increasing the concentration to 2 μM, the inhibition of cells in G2/M was further increased to 56.48%±2.43 and 59.29%±3.87 respectively (Figure 2 and Table 3).

DNA topo I inhibition study: DNA is an essential biological macromolecule and topoisomerase enzymes control its topology. topo I has been identified as the potential target of several anticancer drugs used clinically today, because overproduction of topo I was observed in cancer cells compared to normal cells and they can be categorized as either suppressors or poisons based on the manner in which they interfere with these enzymes. (29) Previous studies indicate that most of the β-carboline derivatives could interact with DNA and inhibit some of the nuclear enzymes involved in DNA processing, such as the activity of topoisomerase. In this context, to study whether this class of compounds target topo I in the fashion similar to our hypothesis, we performed the DNA relaxation assay induced by topo I for the most of the active compounds 10a, 10e and 10u using camptothecin as a positive control. The results obtained in the assay are shown in Figure. 3. Compounds 10a, 10e, and 10u has shown good topo I inhibitory activity at 25 μM, and their inhibition ability was similar to that of camptothecin, a well-known topo I inhibitor. Hence, due to the topo I activity inhibition by 10a, 10e, and 10u compounds, observed increase in the intensity of the band corresponding to the supercoiled DNA. Compounds 10a,10e showed comparatively better topo I inhibition compared to **10u**. In the present study, from the topo I inhibition assay it is clear that the test conjugates namely 10a, 10e and 10u inhibit topo I, like Camtothesin (CPT). CPT is a pentacyclic alkaloid and it will inhibit Top1 activity. (30, 31) The reported mechanism for CPT anticancer activity in a cell is it integrates with DNA and forms topo1/DNA covalent ternary complex. CPT requires both topo1 and DNA for binding, but in the absence of either DNA or topo I, CPT does not have a significant binding. (32) CPT binds to both the topo I enzyme and DNA strand through hydrogen bonding, and prevents both the religation of the nicked DNA as well as dissociation of topo I from the DNA. This results in breakage of DNA double-strand DNA, which ultimately leads to cell death. From the (Figure 3) it is evident that the test conjugates namely 10a, 10e and 10u are inhibiting more or like CPT, the test conjugates may inhibit topo I in through the same mechanism that is followed by CPT. The results of the present study demonstrate that these compounds inhibit topo I efficiently and therefore they may be useful as potential anticancer agents.

UV-vis studies: It is well-known that due to the planar structure of β-carbolines can bind to DNA and induce DNA damage. In order to evaluate the DNA binding ability of these β-carboline conjugates, the UV-visible spectroscopic studies were performed to understand the preliminary information relating to the binding mode of 10a, 10e and 10u compounds with DNA. UV-visible spectra of compound 10a display a prominent absorption band at 283 nm, compound 10e, 10u displayed two bands at 335 nm and 385 nm respectively. On addition of 10 μM CT-DNA in equal increments to 10 μM 10a, 10e and 10u compounds in DMSO, the absorption band intensities are gradually decreased. Their absorption spectra obtained in the absence and presence of CT-DNA is depicted in (Figure 4). It is observed that the change in intensity of absorption bands by the addition of CT- DNA. This hypochromicity effect is due to the addition of CT-DNA to the compounds, which is a characteristic feature of compounds that interact well with DNA. The decrease in the absorption band intensities of the compounds usually describes the interaction between electronic states of the compounds and DNA bases. (33) Whereas, the extent of hypochromism and red-shift in the drug absorption band generally demonstrates the presence of strong intercalative mode of binding, which involves a strong stacking interaction between an aromatic chromophore and the base pairs of DNA. (34) The observed hypochromic effect indicates that these compounds may bind to DNA and form stable complexes may be through intercalative mode interaction.

Fluorescence studies: The fluorescence spectroscopic studies are yet another useful technique to study the interaction of small molecules with macromolecules like DNA at lower concentrations, as it provides the necessary information about the structural changes in the biomolecules upon interaction.[35] Further to understand the binding nature of these compounds 10a, 10e and 10u with DNA, we performed fluorescent titrations at 25 °C as shown in (Figure 5). The intrinsic fluorescence of β-carboline alkaloids is extremely sensitive to its surrounding environment. Hence the interaction of these compounds with CT-DNA could deliver certain observations with regard to the nature of their interaction with DNA. In the present study, the emission spectra of 10a, 10e and 10u in the absence and presence of increasing amounts of CT-DNA were recorded to determine the interaction between these compounds and CT-DNA. (Figure 5) indicates the concentration dependent quenching of compounds fluorescence by CT-DNA, thereby suggesting that there is considerable interaction between these compounds and CT-DNA. The fluorescence intensity of the test compounds gradually enhanced by increasing the concentration of CT-DNA due to the exchange of fluorescence energy between the DNA bases and the compounds. (36) Hyperchromicity of the fluorescence emission peak for 10a, 10e and 10u were observed at 317 nm, 330, nm and 306 nm respectively. Fluorescence spectroscopic results revealed that these compounds bind to DNA in such a manner that they will come closer to the DNA bases. As they come closer, exchange of fluorescence energy takes place between the DNA bases and the compounds. Among these, compound 10u displays the extent of enhancement of emission band intensities may be due to its higher level of interaction with CT-DNA.

Circular dichroism spectroscopy: The circular dichroism (CD) is a valuable technique to investigate the conformational changes in DNA morphology due to the interaction of DNA with small molecules or changes in the environmental conditions. In order to evaluate the interaction effect of these **β**-carboline conjugates on DNA, CD spectroscopy studies were carried out and the results are displayed in Figure 6. The CD spectrum of the calf thymus DNA (CT-DNA) exhibits a positive band at 275 nm due to π–π base stacking and a negative band at 245 nm due to right-hand helicity that indicates that the CT-DNA exists in the right-hand B form. (37)Upon the addition of 10a, 10e and

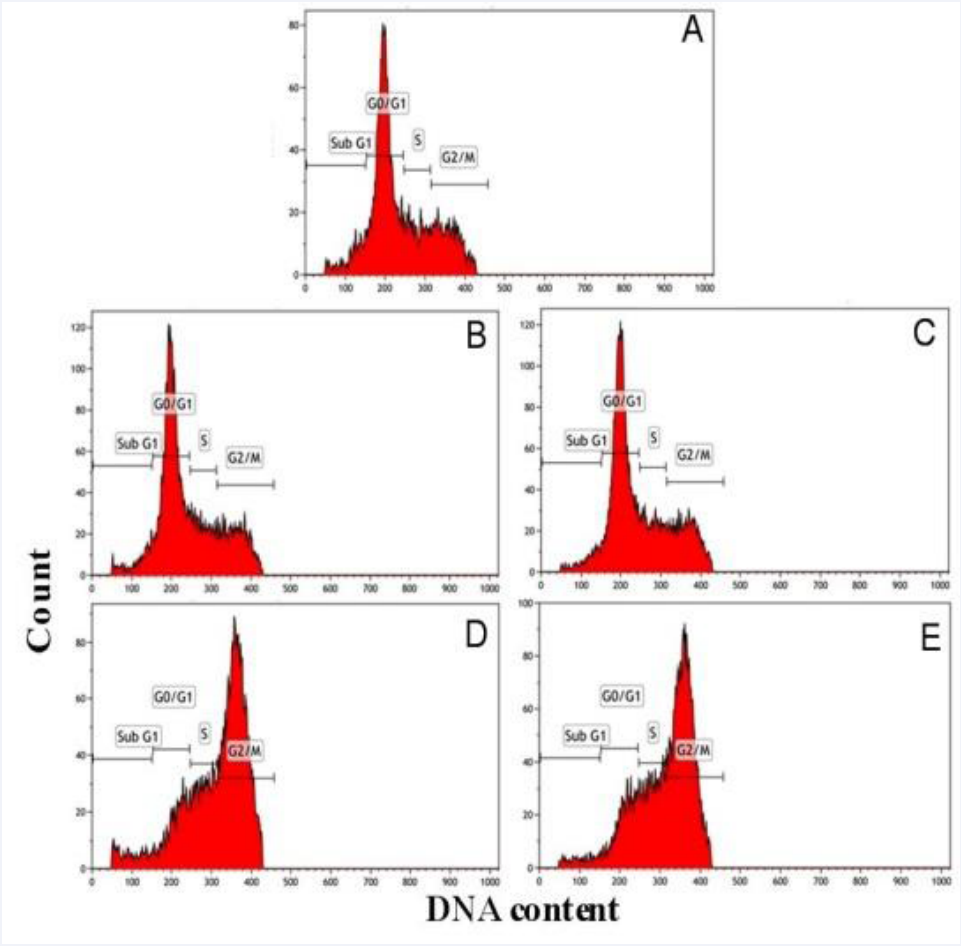

Figure 2 This is the cell cycle histogram obtained when A549 lung cancer cell line; 1 × 105 A549 cells were incubated with derivatives 10a and 10e at 1 and 2 μM concentrations for 48 h. A- Control (A549) (untreated cells); B- 10a (1 μM);C-10a (2 μM); D- 10e (1 μM); E-10e (2 μM).

Sample	Sub G1 %	G0/G1 %	S %	G2/M %
A: Control (A549)	09.15 ±1.03	57.01±3.22	13.48±2.11	20.83±2.11
B: 10a (1 μM)	08.65±1.56	53.14±2.31	17.32±1.35	22.54±2.45
C: 10a (2 μM)	03.66±2.17	16.73±0.93	21.45±2.87	56.48±2.43
D: 10e (1 μM)	07.61±3.11	55.23±2.28	14.42±2.54	24.24±3.22
E: 10e (2 μM)	05.24±2.74	15.17±3.16	19.65±1.33	59.29±3.87

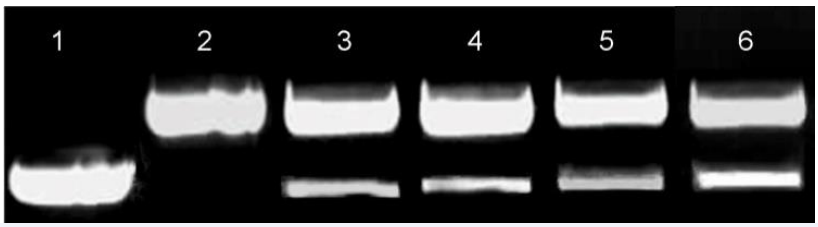

Figure 3 Effect of the selected active compounds 10a, 10e and 10u on Topo I inhibition (Lane 1-DNA alone, Lane 2-DNA + Topo I, Lane 3-DNA + Topo I + 10a, Lane 4-DNA + Topo I + 10e,Lane 5-DNA+Topo I + 10u, Lane 6-DNA+Topo I + camptothecin). In this assay 0.5 μg of DNA was incubated with 1 unit of topo I enzyme and Camptothecin (control) and β-carboline conjugates 10a, 10e and 10u at 25 μM were added to the Topo I-DNA complex and incubated at 37 oC for 30 min.

10u at a concentration of 10 μM to the same concentration of CT DNA solution (DNA: compound, 1:1), positive band at 275 nm exhibits slight hypochromicity, which is an indication of melting of the DNA–compound complex due to the intercalation of the compound with DNA.(38) Further upon increasing the concentration of active compounds (DNA: compound, 1:2) the positive band at 275 nm is further decreased in its intensity, indicating further unwinding of DNA through compounds intercalation. The negative band intensity at 245 nm is altered by the addition of compound, which indicates their ability to

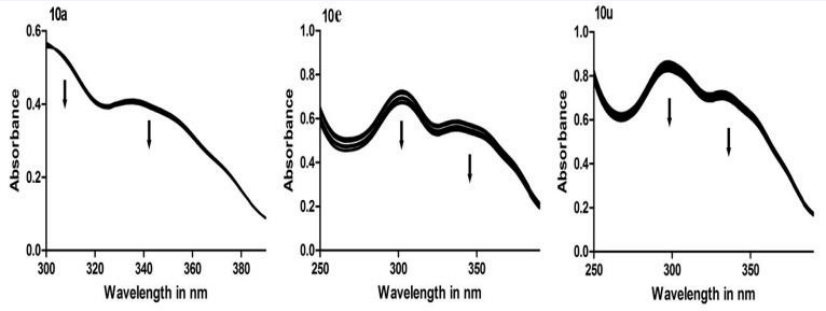

Figure 4 The UV-visible spectra of compounds 10a, 10e and 10u in the absence and presence of increasing concentration of CT-DNA. UV titration was done at 37oC. UV-visible absorption titrations were performed by adding 10 μM CT DNA solution in 100 mM Tris-HCl (pH 7.0). Arrows indicate the change in the absorption spectral intensity upon increasing the concentration of CT-DNA.

bring changes in the DNA helix. From the DNA binding studies, it is evident that these β-carboline conjugates are interacting well with DNA and they bind to DNA through intercalation.

Viscosity studies: Spectroscopic studies provide preliminary information about the nature of binding by these β-carboline conjugates to the DNA. However, these results alone are not sufficient to claim that the intercalative mode of hybrid binding to DNA. To further corroborate the mode of interaction between these compounds and DNA, viscosity measurements were performed with DNA in the absence and presence of compounds. The relative viscosity studies were carried out to have a clear view on the nature of hybrid-DNA interaction. Relative specific viscosity (η/η_0) of DNA is firmly dependent on the length changes that may be associated with the separation of DNA base pairs caused by intercalative/groove binding or electrostatic interaction between DNA's double helix and a small molecules. The intercalated compound cause lengthening of the DNA helix and increases its relative viscosity. Whereas, the groove binding or electrostatically interacting compound links or bends the DNA helix and reduces its effective length and, consequently, it exerts essentially no effect on DNA viscosity.(39) A well-known classical DNA intercalator, ethidium bromide (EtBr) leads to a substantial increase in the relative viscosity of the DNA solutions. Whereas, a well-known groove binder like Hoechst 33342 exhibits minimal or no change in the relative viscosity of the DNA solutions (η and η_0 are the specific viscosities of DNA in the presence and absence of the complexes, respectively). In the present investigation, Hoechst 33342 was taken as a positive control and EtBr was considered as a control. The influences of active compounds (**10a** and **10e)** on the viscosity of CT DNA are displayed in (Figure 7). The viscosity of DNA has increased steadily with the addition of EtBr, whereas minimal change in viscosity of DNA was noticed with the addition of Hoechst 33342. Interestingly, upon the addition of compounds **10a** and **10e** to CT-DNA, the relative viscosity of DNA increases gradually, as in the case of like classical intercalator EtBr. The increment in relative viscosity, anticipated to correlate with the compounds DNA-intercalating potential, EtBr > **10a** > **10e**> Hoechst 33342. Thus, the relative viscosity increment in the DNA caused compounds **10a** and **10e** offer auxiliary support for the intercalative mode of interaction with DNA.

Molecular docking studies: Molecular docking analysis was carried out to identify the potential interaction of these conjugates with the DNA and topo I. The protein structure of human DNA topo I (70 kDa) in complex with the indenoisoquinoline (PDB code: 1SC7, resolution 3.0 Å) was obtained from the RCSB PDB and was prepared using the Protein Preparation Wizard of the Maeströ 9.9. In order to define the correct ionization and tautomeric states of amino acid residues, hydrogen atoms were added to the protein. The Prime module incorporated in Maeströ 9.9 was used to correct the missing side chains of residues. Further, OPLS-2005 force field was used to diminish steric clashes that could possibly exist in the structures under study. The minimization was stopped when the energy converged or the Root Mean Square Deviation (RMSD) reached a maximum cut off of 0.30 Å. Water molecules beyond 5 Å from hetero groups were deleted. Molecular docking studies were performed using Glide, keeping the grid box of size 12 Å from the centroid to cover the entire vicinity of active site. The bound ligand: indenoisoquinoline was re-docked with the active site of human DNA topo I for validation of the docking protocol. It gave GLIDE score of -9.741 and showed hydrogen bond with Arg364 and Asn722 along with π-stacking interaction with TGP11 and hydrophobic interactions with Leu721 (Figure 8A). Once the docking protocol was validated, all the compounds from the synthesized library were docked into the active site. Amongst them, the hydrogen bonding and hydrophobic interactions shown by the most active compounds 10a, 10e and 10u with DNA as well as topo I are elaborated. Compound 10a gave GLIDE score of -8.868. The O-atom of quinazolin-4-one forms H- bonding with TGP11 and π-stacking interaction with DA113 and TGP11. Hydrophobic interactions are seen with Ala351, Met428 and Ala715. The oligonucleotide sequence of the cleavable strand of the duplex oligomer along with our compound is 5'– AAAAAGACTT-bc-XGAAAATTTTT-3', where, 'bc' represents the compound intercalating with the DNA and 'X' represents TGP. Similarly**,** 10e and 10u gave GLIDE scores of -8.508 and -7.305 respectively. The receptor-ligand interactions are shown in (Figure 8) and the 3D binding poses along with interactions are represented in (Figure 9) the molecular docking results indicate that these compounds interact with the DNA via intercalation, which was shown in (Figure 10). A full view of topo 1 and DNA intercalation is shown in (Figure 11).

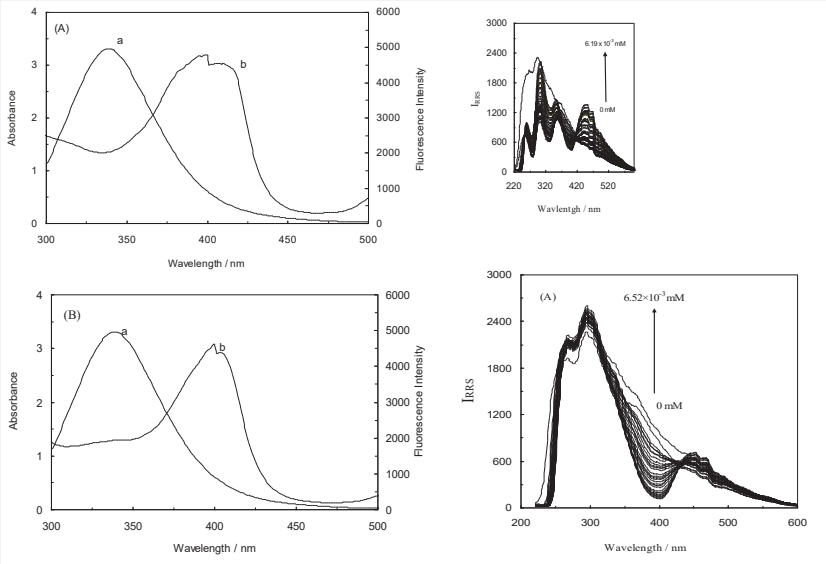

Figure 5 Fluorescence spectra of compounds 10a, 10e and 10u in the absence or presence of increasing amounts of CT-DNA. The experiments were done at 37oC. To the fixed concentration compounds (10 μM), CT-DNA was added in regular intervals (each addition with an increment of 0.1 μM CT-DNA). Arrows indicate the change in emission intensity upon increasing the concentration of CT-DNA.

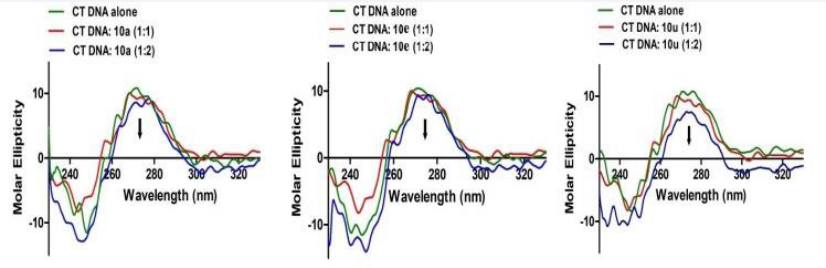

Figure 6 CD spectra of compounds 10a, 10e and 10u with CT-DNA in the absence and presence of increasing amounts of test conjugates. In CD experiment, the concentration of CT DNA was kept constant and the test conjugates were added at 1:1 and 1:2 ratios to find the changes in the conformation of CT-DNA with the interaction of test conjugates.

MATERIAL AND METHODS

Chemistry

2-Methyl-6-nitro-4*H*-benzo[*d*][1,3]oxazin-4-one (2): A solution of 5- nitroanthranilicacid (**1**, 1 mol) and acetic anhydride (5 ml) was stirred at 150 °C for 1 h. Then, reaction mixture was cooled to room temperature and excess amount of acetic anhydride was removed in *vacuo*. The obtained crude product was washed with hexane and dried under reduced pressure. The product was directly used for next step without any further purification. Light yellow solid; Yield: 90%.

General reaction procedure for the preparation of compounds (3a-g)

To a stirred solution of compound **2** (1 mmol) in acetic acid, substituted anilines (1 mmol) are added and the mixture was stirred at 150 °C for 4 h until complete consumption of starting materials monitored by TLC. Then, the mixture was cooled to room temperature and excess amount of acetic acid was removed in *vacuo*, and obtained crude was basified with saturated $NaHCO_3$ solution and extracted with excess amount of CH_2Cl_2. Then, the combined organic layer was washed with water, brine solution and dried over anhydrous Na_2SO_4 and concentrated under reduced pressure. Then, the obtained solid recrystallized to afford products **9a–g** with high purity.

3-(2-Methoxyphenyl)-2-methyl-6-nitroquinazolin-4(3H)-one (3a): White solid; Yield: 78%; Mp: 174–176 °C; ^{1}H NMR (500 MHz, $CDCl_3$) δ: 9.12 (d, *J* = 2.6 Hz, 1H), 8.54 (dd, *J* = 2.6, 8.8 Hz, 1H), 7.78 (d, *J* = 9.0 Hz, 1H), 7.54–7.50 (m, 1H), 7.22 (dd, *J* = 1.7, 7.6 Hz, 1H), 7.16 (dd, *J* = 1.2, 7.6 Hz, 1H), 7.14–7.11 (m, 1H), 3.82 (s,3H), 2.28 (s, 3H) ; ^{13}C NMR ($CDCl_3$, 125 MHz) δ: 160.6, 158.9, 154.2, 151.7, 145.3, 131.3, 128.9, 128.4, 128.3, 125.6, 123.7, 121.5, 120.9, 112.3, 55.7, 23.7; MS (ESI): *m/z* 312 [M + H]$^+$; HRMS (ESI): *m/z* calcd for $C_{16}H_{14}O_4N_3$: 312.09788; found: 312.09803 [M + H]$^+$.

3-(3-Methoxyphenyl)-2-methyl-6-nitroquinazolin-4(3H)-one (3b): White solid; Yield: 81%; Mp: 176–178 °C; ^{1}H NMR (300 MHz, $CDCl_3$) δ: 9.07 (t, *J* = 2.3 Hz, 1H), 8.55–8.50 (m, 1H), 7.77 (d, *J* = 9.1 Hz, 1H), 7.50 (t, *J* = 8.1 Hz, 1H), 7.08(dd, *J* =

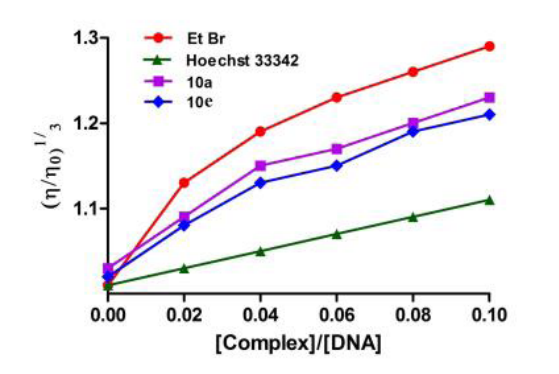

Figure 7 This assay is done to find the nature of interaction of test conjugates namely 10a and 10e with CT-DNA. The experiment was done at 37oC Effect of increasing amounts of EtBr, Hoechst 33342 and compounds 10a and 10e on the relative viscosity of CT-DNA.

1,9, 8.5 Hz, 1H), 6.86 (d, *J* = 7.7 Hz, 1H), 6.81 (t, *J* = 2.1 Hz, 1H), 3.86 (s, 3H), 2.34 (s, 3H); ^{13}C NMR (125 MHz, $CDCl_3$) δ: 160.9, 160.8, 158.0, 151.4, 145.4, 137.8, 130.9, 128.5, 128.4, 123.6, 120.8, 119.6, 115.3, 113.5, 55.5, 24.4; MS (ESI): *m/z* 312 $[M + H]^+$; HRMS (ESI): *m/z* calcd for $C_{16}H_{14}O_4N_3$: 312.09788; found: 312.09824 $[M + H]^+$.

3-(4-Methoxyphenyl)-2-methyl-6-nitroquinazolin-4(3H)-one (3c): White solid; Yield: 82%; Mp: 181–183 °C; ^{1}H NMR (500 MHz, $CDCl_3$) δ: 9.11 (d, *J* = 2.7 Hz, 1H), 8.54 (dd, *J* = 2.6, 9.0 Hz, 1H), 7.78 (d, *J* = 9.0 Hz, 1H), 7.20–7.16 (m, 2H), 7.10–7.06 (m, 2H), 3.89 (s, 3H), 2.32 (s, 3H); ^{13}C NMR (125 MHz, $CDCl_3$) δ: 161.2160.2, 158.6, 151.5, 145.4, 129.2, 128.6, 128.5, 128.4, 123.7, 120.9, 115.4, 55.5, 24.6; MS (ESI): *m/z*

312 $[M + H]^+$; HRMS (ESI): *m/z* calcd for $C_{16}H_{14}O_4N_3$: 312.09788; found: 312.09803 $[M + H]^+$.

2-Methyl-6-nitro-3-(m-tolyl)quinazolin-4(3H)-one (3d): White solid; Yield: 79%; Mp: 187–189 °C;^{1}H NMR (300 MHz, $CDCl_3$) δ: 9.12 (d, *J* = 2.3 Hz, 1H), 8.55 (dd, *J* = 2.3,9.1 Hz, 1H), 7.79 (d, *J* = 9.1 Hz, 1H), 7.48 (t, *J* = 7.5 Hz, 1H), 7.36 (d, *J* = 7.5 Hz, 1H), 7.10–7.04 (m, 2H), 2.45 (s, 3H), 2.31 (s, 3H); ^{13}C NMR (75 MHz,

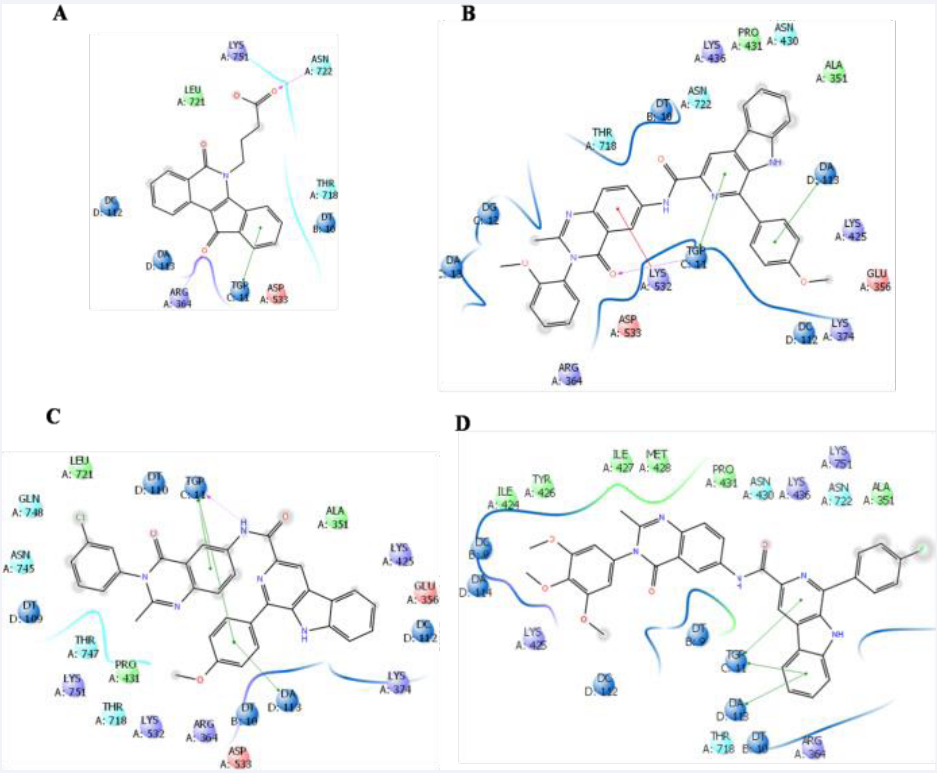

Figure 8 Receptor-ligand interaction diagram (2D view) of Co-crystal (A), 10a (B), 10e (C) and 10u (D) at active binding site of Human DNA Topoisomerase (PDB code: 1SC7). Amino acid residues within 4 Å of the ligand are presented in the 2D interaction diagram. The pink and green colour arrow lines represent hydrogen bonding and π-π interactions, respectively, whereas the red line indicates π-cation interactions.

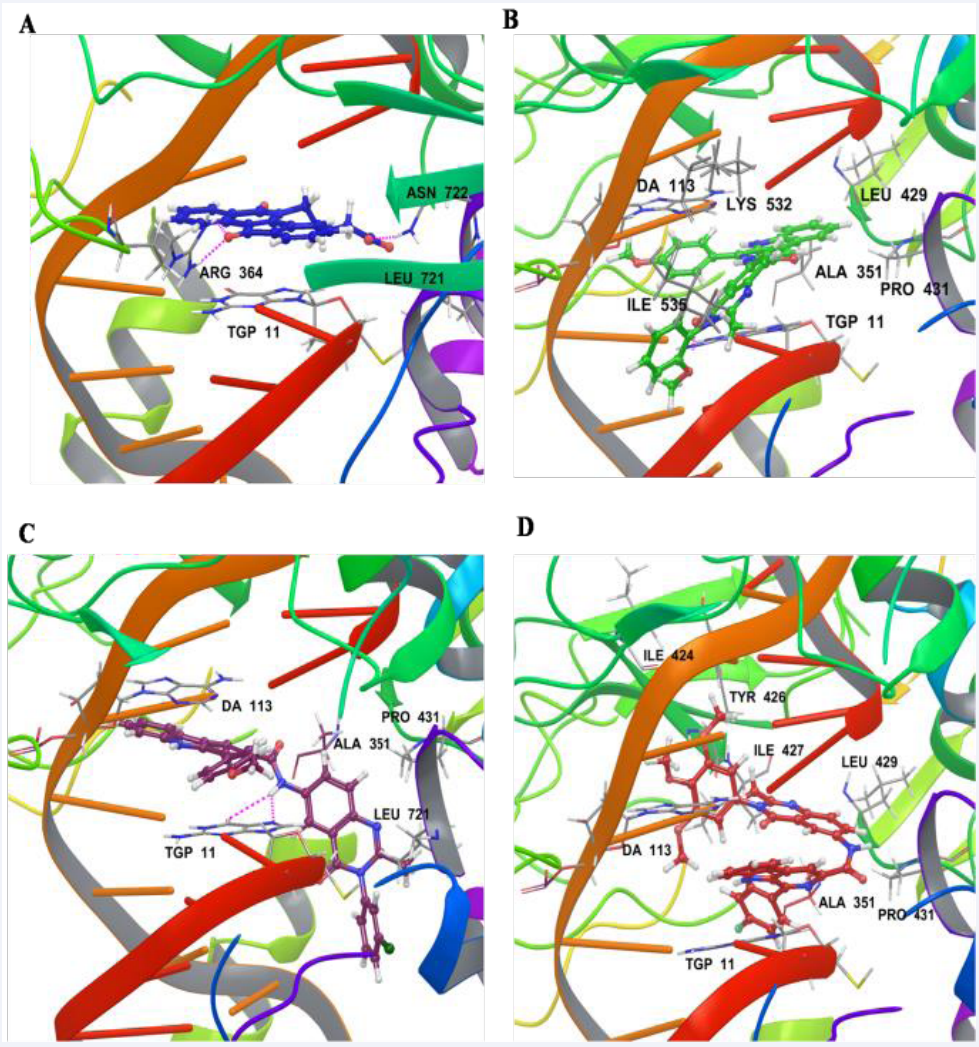

Figure 9 Binding pose, hydrogen bonds and hydrophobic interactions of co-crystal–indenoisoquinoline (A), compounds 10a (B), 10e (C) and 10u (D) with DNA-Topoisomerase I (PDB code: 1SC7). Co-crystal is indicated in blue coloured ball and stick, whereas compounds 10a, 10e and 10u are represented as green, maroon and red coloured ball and stick models, respectively. The pink colour lines represent hydrogen bonding.

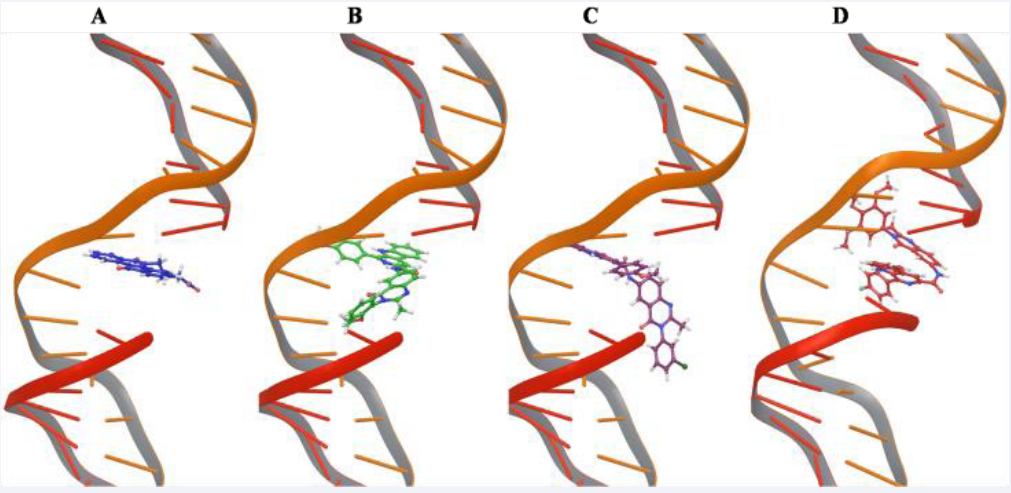

Figure 10 Binding poses of co-crystal-indenoisoquinoline (A), compounds 10a (B), 10e (C) and 10u (D) with the human DNA showing their intercalation.

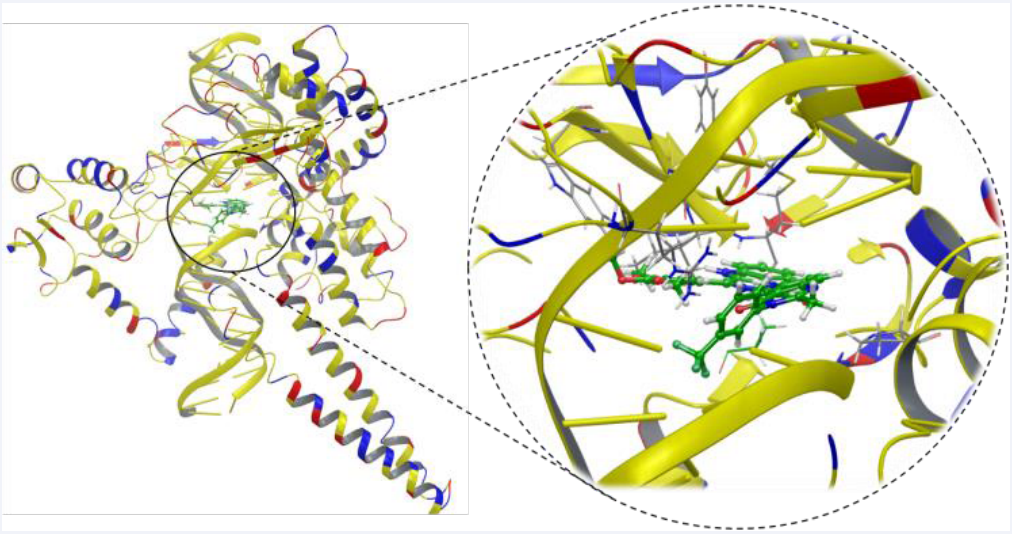

Figure 11 The molecular docking image showing the full view of Topo 1 and DNA intercalation.

$CDCl_3$) δ: 161.1, 158.3, 151.6, 145.5, 140.6, 136.8, 130.6, 131.1, 128.6, 128.5, 128.1, 124.6, 123.7, 120.9, 24.7, 21.4; MS (ESI): *m/z* 296 [M + H]$^+$; HRMS (ESI): *m/z* calcd for $C_{16}H_{14}O_3N_3$: 296.10297; found: 296.10332 [M + H]$^+$.

3-(3-Chlorophenyl)-2-methyl-6-nitroquinazolin-4(3H)-one (3e): White solid; Yield: 77%; Mp: 207–209 °C; ^{1}H NMR (500 MHz, $CDCl_3$) δ: 9.06 (d, *J* = 2.3 Hz, 1H), 8.54 (dd, *J* = 3.0,9.1 Hz, 1H), 7.79 (d, *J* = 8.3 Hz, 1H), 7.55 (d, *J* = 5.3 Hz, 2H), 7.33 (s, 1H), 7.24–7.18 (m, 1H), 2.33 (s, 3H); ^{13}C NMR (125 MHz, $CDCl_3$) δ: 160.7, 157.4, 153.3, 145.5, 137.8, 135.8, 131.2, 130.1, 128.7, 128.5, 128.1, 126.1, 123.5, 120.9, 24 .6; MS (ESI): *m/z* 316 [M + H]$^+$; HRMS (ESI): *m/z* calcd for $C_{15}H_{11}O_3N_3Cl$: 316.04835; found: 316.04875 [M + H]$^+$.

2-Methyl-6-nitro-3-(3-(trifluoromethyl)phenyl) quinazolin-4(3H)-one (3f): White solid; Yield:75%; Mp: 196–198 °C;^{1}H NMR (500 MHz, $CDCl_3$) δ: 9.06 (d, *J* = 2.6 Hz, 1H), 8.55 (dd, *J* = 2.6,9.0 Hz, 1H), 7.84 (d, *J* = 7.9 Hz, 1H), 7.80 (d, *J* = 9.0 Hz, 1H), 7.77 (t, *J* = 7.9 Hz, 1H), 7.59 (s, 1H), 7.52 (d, *J* = 7.9 Hz, 1H), 2.31 (s, 3H); ^{13}C NMR ($CDCl_3$, 75 MHz) δ: 160.8, 157.1, 152.3, 145.6, 137.4, 133.1, 132.6, 131.5, 131.0, 128.9, 128.6,127.0, 125.0, 123.5,120.6, 24.6; MS (ESI): *m/z* 350 [M + H]$^+$; HRMS (ESI): *m/z* calcd for $C_{16}H_{11}O_3N_3F_3$: 350.07470; found: 350.07521 [M + H]$^+$.

2-Methyl-6-nitro-3-(3,4,5-trimethoxyphenyl)quinazolin-4(3H)-one (3g): White solid; Yield: 84%; Mp: 195–197 °C; ^{1}H NMR (300 MHz, $CDCl_3$) δ: 9.04 (d, *J* = 2.3 Hz,1H), 8.52 (dd, *J* = 3.0, 9.0 Hz, 1H), 7.77 (d, *J* = 9.0 Hz, 1H) 6.51 (s, 3H), 3.91 (s 3H), 3.88 (s, 6H), 2.39 (s, 3H); ^{13}C NMR (75 MHz, $CDCl_3$) δ: 161.0, 158.3, 154.3, 151.3, 145.3, 138.6, 132.2, 128.6, 128.4, 123.5, 120.7, 104.7, 60.7, 56.2, 24.3; MS (ESI): *m/z* 372 [M + H]$^+$; HRMS (ESI): *m/z* calcd for $C_{18}H_{18}O_6N_3$: 372. 11901; found: 372.11947 [M + H] $^+$.

General reaction procedure for the preparation of compounds (4a-g)

To a stirred solution of **3a-g** (1 mmol) in MeOH and water (2:1) was added **Fe** (5 mmol) and NH_4Cl (10 mmol) and stirred at 100 °C for 3 h until complete consumption of starting materials monitored by TLC. Then the MeOH was removed in *vacuo* and the obtained crude was diluted with CH_2Cl_2, which was filtered through celite and celite bed was washed with CH_2Cl_2. The combined organic layer was washed with water as well saturated brine solution, dried over anhydrous sodium sulphate and concentrated under pressure. Then, the obtained solid was recrystallized to afford pure products 4a-g.

6-Amino-3-(2-methoxyphenyl)-2-methylquinazolin-4(3H)-one (4a): Yellow solid; Yield: 86%; Mp: 176–178 °C; ^{1}H NMR (300 MHz, DMSO–d_6) δ: 7.49 (t, *J* = 8.9 Hz, 1H), 7.34 (d, *J* = 8.5 Hz, 2H), 7.23 (d, *J* = 7.7 Hz, 1H), 7.16 (d, *J* = 2.5Hz, 1H),7.14–7.05 (m, 2H), 5.58 (s, 2H), 3.75 (s, 3H), 2.0 (s, 3H); ^{13}C NMR (100 MHz, DMSO–d_6) δ: 161.0, 159.9, 148.6, 147.5, 139.5, 138.2, 130.0, 127.3, 122.3, 121.2, 120.4, 114.3, 114.1, 106.5, 55.2, 23.2; MS (ESI): m/z 282 [M + H]$^+$; HRMS (ESI): *m/z*: calcd for $C_{16}H_{16}O_2N_3Na$: 304.10565; found: 304.10536 [M + H]$^+$.

6-Amino-3-(3-methoxyphenyl)-2-methylquinazolin-4(3H)-one (4b) Yellow solid; Yield: 87% yield; Mp: 179–181 °C;^{1}H NMR (300 MHz, DMSO–d_6) δ: 7.45 (t, *J* = 7.9 Hz, 1H), 7.36 (d, *J* = 8.7 Hz, 1H), 7.18 (d, *J* = 2.5 Hz, 1H), 7.11–7.0 (m, 3H), 6.94 (d, *J* = 7.7 Hz, 1H), 5.58 (s, 2H), 3.79 (s, 3H), 2.07 (s, 3H); ^{13}C NMR (75 MHz, $CDCl_3$ + DMSO–d_6) δ: 161.1, 159.8, 148.9, 145.8, 138.5, 138.4, 129.7, 126.8, 122.4, 120.7, 119.4, 113.9, 113.0, 107.5, 54.6, 22.8; MS (ESI): *m/z* 282 [M + H]$^+$; MS (ESI): m/z 282 [M + H]$^+$; HRMS (ESI): *m/z*: calcd for $C_{16}H_{16}O_2N_3Na$: 304.10565; found: 304.10542 [M + H]$^+$.

6-Amino-3-(4-methoxyphenyl)-2-methylquinazolin-4(3*H*)-one (4c): Yellow solid; Yield: 90%; Mp: 183–185 °C; ^{1}H NMR (500 MHz, $CDCl_3$) δ: 7.51 (d, *J* = 9.1 Hz, 1H), 7.45 (d, *J* = 2.3 Hz, 1H), 7.18–7.09 (m, 3H), 7.07–7.02 (m, 2H), 4.18–3.89 (s, 2H),3.87 (s, 3H), 2.21 (s, 3H); ^{13}C NMR (75 MHz, DMSO–d_6) δ: 161.4, 159.0, 149.2, 147.5, 138.2, 130.7, 129.4, 127.3, 122.3, 121.3, 114.5, 106.5, 55.3 23.5; MS (ESI): *m/z* 282 [M + H]$^+$. MS (ESI): *m/z* 282 [M + H]$^+$; HRMS (ESI): *m/z*: calcd for $C_{16}H_{16}O_2N_3Na$: 304.10565; found: 304.10536 [M + H]$^+$.

6-Amino-2-methyl-3-(*m*-tolyl)quinazolin-4(3*H*)-one (4d): Yellow solid; Yield: 86%; Mp: 180–182 °C;^{1}H NMR (500 MHz, $CDCl_3$) δ: 7.51 (d, *J* = 8.5 Hz, 1H), 7.45 (d, *J* = 2.7 Hz, 1H), 7.42 (t, *J* = 7.9 Hz, 1H), 7.29 (d, *J* = 7.6 Hz, 1H), 7.11 (dd, *J* = 2.7, 8.7 Hz, 1H), 7.07–7.03 (m, 2H), 4.10–3.84 (bs, 2H), 2.42 (s, 3H), 2.20 (s, 3H); ^{13}C NMR (75 MHz, DMSO–d_6) δ: 6161.1, 148.6, 147.5, 138.9, 138.2, 138.1, 129.2, 129.1, 128.7, 127.3, 125.3, 122.3, 121.1, 106.5, 23.4, 20.7; MS (ESI): *m/z* 266 [M + H]$^+$; HRMS (ESI): *m/z*: calcd for $C_{16}H_{16}ON_3Na$: 266.12879; found: 266.12872 [M + H]$^+$.

6-Amino-3-(3-chlorophenyl)-2-methylquinazolin-4(3*H*)-one (4e): Yellow solid; Yield: 84%; Mp: 221–223 °C; ^{1}H NMR (500 MHz, $CDCl_3$) δ: 7.52–7.47 (m, 3H), 7.43 (d, *J* = 2.7 Hz, 1H), 7.31–7.28 (m, 1H), 7.19–7.15 (m, 1H), 7.12 (dd, *J* = 2.7, 8.4 Hz, 1H), 4.9–3.82 (s, 1H), 2.21 (s, 3H); ^{13}C NMR (75 MHz, DMSO–d_6) δ: 161.1, 148.2, 147.6, 139.6, 138.1, 133.4, 130.9, 128.8, 128.7, 127.5, 127.4, 122.4, 121.1, 106.5, 23.4; MS (ESI): *m/z* 286 [M + H]$^+$; HRMS (ESI): *m/z*: calcd for $C_{15}H_{13}ON_3Cl$: 286.07417; found: 286.07410 [M + H]$^+$.

6-Amino-2-methyl-3-(3-(trifluoromethyl) phenyl) quinazolin-4(3*H*)-one (4f): Yellow solid; Yield: 82%; Mp: 168-170 °C; ^{1}H NMR (300 MHz, DMSO–d_6) δ: 7.94 (s, 1H), 7.88 (d, *J* = 6.9 Hz, 1H), 7.83–7.71 (m, 2H), 7.38 (d, *J* = 8.6 Hz, 1H), 7.18 (d, *J* = 2.5 Hz, 1H), 7.10 (dd, *J* = 8.6, 2.6 Hz, 1H), 5.62 (s, 2H), 2.03 (s, 3H); ^{13}C NMR (75 MHz, DMSO–d_6) δ: 161.4, 148.3, 147.7, 139.1, 138.3, 133.1, 130.8, 130.3 (dd, *J* = 32.5, 64.9 Hz), 127.5, 125.7 (dd, *J* = 14.1, 3.4 Hz), 125.6, 122.6, 122.0, 121.2, 106.6, 23.6; MS (ESI): *m/z* 320 [M + H]$^+$; HRMS (ESI): *m/z*: calcd for $C_{16}H_{13}ON_3F_3$: 320.10052; found: 320.10026 [M + H]$^+$.

6-Amino-2-methyl-3-(3,4,5-trimethoxyphenyl) quinazolin-4(3*H*)-one (4g): Pale yellow solid: 92% yield; Mp: 186–188 °C; ^{1}H NMR (300 MHz, $CDCl_3$) δ: 7.52 (d, *J* = 8.7 Hz, 1H), 7.45 (d, *J* = 2.6 Hz, 1H), 7.13 (dd, *J* = 2.6, 8.7 Hz, 1H), 6.48 (s, 2H), 3.92 (s, 3H), 3.86 (s, 6H), 2.27 (s, 3H); ^{13}C NMR (75 MHz, $CDCl_3$) δ: 162.1, 153.9, 150.5, 145.5, 140.0, 138.1, 133.5, 127.8, 123.3, 121.5, 109.0, 105.2, 60.8, 56.1, 23.5; MS (ESI): *m/z* 342 [M + H]$^+$; HRMS (ESI): *m/z*: calcd for $C_{18}H_{19}O_4N_3Na$: 364.12678; found: 364.12659 [M + H]$^+$.

Preparation of (*S*)-Methyl 2-amino-3-(1H-indol-3-yl) propanoate (6)

To a stirred solution of L-tryptophan (**5**, 10 mmol) in methanol (5 mL), thionyl chloride (11 mmol) was added drop-wise at 0 °C and continued stirring for 12 h at room temperature until complete consumption monitored by TLC. The excess amount of solvent was removed under reduced pressure and the resulting mixture was diluted with dry acetone (5 mL) and filtered, dried to obtain L-tryptophan methyl ester hydrochloride salt as white solid (**2**), which was directly used for the next step without any further purification.

General reaction procedure for the synthesis of tetrahydro-β-carboline esters 8a-d: To a mixture of L–tryptophan ester hydrochloride salt (**6**, 1 mmol) and substituted benzaldehyde (1 mmol) in EtOH was stirred at reflux temperature for 12 h. After completion of the reaction, solvent was removed *in vacuo* and the crude product **6a-d** (1 mmol) was taken in dry DMF and Et_3N (3 mmol), and a solution of TCCA (1.1 mmol) in DMF was added drop wise at −20 °C. Then the reaction mixture was allowed slowly to 0 °C and stirred at the same temperature for 2 h. After the completion of reaction monitored by TLC, reaction mixture was quenched with ice water. The obtained precipitate was filtered, washed with water, and dried *in vacuo* to give the compounds **8a–d**.

Methyl 1-(4-methoxyphenyl)-9*H*-pyrido[3,4-*b*]indole-3-carboxylate (8a): White solid; Yield: 83%; Mp: 228–230 °C; ^{1}H NMR (300 MHz, $CDCl_3$ + DMSO–d_6) δ: 11.66 (s, 1H), 8.79 (s, 1H), 8.22 (d, *J* = 7.9 Hz, 1H), 8.00 (d, *J* = 8.7 Hz, 2H), 7.69 (d, *J* = 8.2 Hz, 1H), 7.55 (dd, *J* = 11.3, 4.0 Hz, 1H), 7.31 (t, *J* = 7.5 Hz, 1H), 7.11 (d, *J* = 8.7 H 2H), 3.99 (s, 3H), 3.90 (s, 3H); ^{13}C NMR (75 MHz, $CDCl_3$ + DMSO–d_6) δ: 171.4, 165.0, 147.34, 146.6, 141.7, 139.8, 135.3, 135.0, 134.1, 133.3, 126.4, 126.4, 125.3, 121.1, 118.9, 117.8, 60.2, 57.1; MS (ESI): *m/z* 333 [M + H]$^+$; HRMS (ESI): *m/z* calcd for $C_{20}H_{17}O_3N_2$: 333.12337; found: 333.12194 [M + H]$^+$.

Methyl 1-(*p*-tolyl)-9*H*-pyrido[3,4-*b*]indole-3-carboxylate (8b): White solid; Yield: 80%; Mp: 192–194 °C; ^{1}H NMR (300 MHz, $CDCl_3$ + DMSO–d_6) δ: 8.89 (s,1H), 8.40 (d, *J* = 7.9 Hz, 1H), 7.92 (d, *J* = 8.0 Hz, 1H), 7.70 (d, *J* = 8.2 Hz, 1H), 7.60 (t, *J* = 7.6 Hz, 1H), 7.44 (d, *J* = 7.9 Hz, 1H), 7.32 (t, *J* = 7.4 Hz, 1H), 3.93 (s, 1H), 2.44 (s, 1H); ^{13}C NMR (75 MHz, $CDCl_3$ + DMSO–d_6) δ: 171.3, 147.4, 146.7, 143.7, 141.8, 139.9, 139.7, 134.6, 134.3, 133.8, 133.7, 127.2, 126.4, 125.6, 121.73, 118.0, 57.3, 26.2; MS (ESI): *m/z* 317 [M + H]$^+$; HRMS (ESI): *m/z* calcd for $C_{20}H_{17}O_2N_2$: 317.12845; found: 317.12788 [M + H]$^+$.

Methyl 1-(4-fluorophenyl)-9*H*-pyrido[3,4-*b*]indole-3-carboxylate (8c): White solid: yield; 78%; Mp: 195–198 °C; ^{1}H NMR (500 MHz, $CDCl_3$) δ: 8.87 (s, 1H), 8.83 (s, 1H), 8.22 (d, *J* = 7.9 Hz, 1H), 7.92 (dd, *J* = 8.7, 5.3 Hz, 2H), 7.61 (s, 1H), 7.57 (s, 1H), 7.39 (s, 1H), 7.24–7.18 (m, 2H), 4.06 (s, 3H); ^{13}C NMR (75 MHz, $CDCl_3$ + DMSO– d_6) δ: 165.7, 162.39 (d, *J* = 246.8 Hz), 141.3, 140.8, 136.4, 134.3, 133.77 (d, *J* = 2.6 Hz), 130.49 (d, *J* = 8.4 Hz), 129.0, 128.2, 121.4, 120.9, 120.1, 116.3, 115.23 (d, *J* = 21.5 Hz), 112.5, 51.7; MS (ESI): *m/z* 321 [M + H]$^+$; HRMS (ESI): *m/z* calcd for $C_{19}H_{14}O_2N_2F$: 321.10338; found: 321.10298 [M + H]$^+$.

Methyl 1-(3,4,5-trimethoxyphenyl)-9*H*-pyrido[3,4-*b*] indole-3-carboxylate (8d): 1H), 7.52–7.44 (m, 1H), 7.25 (t, *J* = 7.2 Hz, 1H), 7.15 (s, 2H), 3.95 (s, 3H), 3.90 (s, 6H), 3.81 (s, 3H); ^{13}C NMR (75 MHz, $CDCl_3$ + DMSO–d_6) δ: 165.8, 152.8, 142.2, 141. 137.8, 136.2, 134.5, 132.9, 128.7, 128.0, 121.1, 121.0, 119.9, 116.1, 112.5, 105.6, 59.9, 55.5, 51.7; MS (ESI): *m/z* 393 [M + H]$^+$; HRMS (ESI): *m/z* calcd for $C_{22}H_{21}O_5N_2$: 393.14450; found: 393.14320 [M + H]$^+$.

General reaction procedure for the synthesis of tetrahydro-β-carboline acids 9a-d

To a stirred solution of compound **8a-d** (1 mmol) in MeOH was added aqueous solution of NaOH (2 mmol) and stirred for 6 h at 70 °C until complete consumption of starting materials monitored by TLC. After completion of the reaction, MeOH was evaporated *in vacuo* and the obtained residue was acidified with 10% citric acid solution and the resulted precipitate was filtered, washed with ethanol and dried. These well dried solid products **9a-d** were employed directly for next step without any further purification.

General reaction procedure for the synthesis of C3 quinazolinone linked β-carboline congeners 10a-z, 10aa and 10ab

To a stirred solution of compound 9a-d (1 mmol) and compound 4a-g (1 mmol) in CH_2Cl_2 were added EDCI (1.2 mmol), HOBt (1.2 mmol) and TEA (3 mmol) at 0 °C and stirred at room temperature for 12 h until complete consumption of starting materials monitored by TLC. The reaction mixture was quenched with ice cold water and extracted with CH_2Cl_2, the combined organic phases were dried over Na_2SO_4 and concentrated under reduced pressure to get crude products, which were purified by silica gel column chromatography by using EtOAc/hexane as eluent.

1-(4-Methoxyphenyl)-*N*-(3-(2-methoxyphenyl)-2-methyl-4-oxo-3,4-dihydroquinazolin-6-yl)-9*H*-pyrido[3,4-*b*]indole-3-carboxamide (10a): Off white solid; Yield; 88%; Mp: 316–318 °C; 1H NMR (300 MHz, CDCl3 + DMSO–d6) δ: 10.71 (s, 1H), 8.88 (s, 1H), 8.72 (s, 1H), 8.32 (d, J = 7.9 Hz, 1H), 8.27 (dd, J = 1.7, 8.8 Hz, 1H), 8.19 (d, J = 8.6 Hz, 2H), 7.74–7.60 (m, 2H), 7.58–7.45 (m, 2H), 7.36–7.25 (m, 2H), 7.24–7.07 (m, 4H), 3.90 (s, 3H), 3.78 (s, 3H), 2.11 (s, 3H); 13C NMR (75 MHz, CDCl3 + DMSO–d6) δ: 163.1, 160.6, 159.7, 153.9, 152.9, 143.2, 141.4, 141.3, 140.4, 138.4, 136.4, 134.2, 130.2, 129.7, 1295, 129.0, 127.9, 126.7, 126.6, 125.7, 121.1, 120.9, 120.6, 120.4, 119.8, 115.5, 114.4, 113.7, 112.5, 111.9, 55.3, 54.9, 22.7; MS (ESI): m/z 582 [M + H]+; HRMS (ESI): m/z calcd for C35H28O4N5: 582.21358; found: 582.21431 [M + H]+.

1-(4-Methoxyphenyl)-*N*-(3-(3-methoxyphenyl)-2-methyl-4-oxo-3,4-dihydroquinazolin-6-yl)-9*H*-pyrido[3,4-*b*]indole-3-carboxamide (10b): White solid; Yield: 89%; Mp: 206–208 °C; ^{1}H NMR (300 MHz, $CDCl_3$ + DMSO–d_6) δ: 11.52 (s, 1H), 10.62 (s, 1H), 8.90 (s, 1H), 8.58(d, *J* = 2.2 Hz, 1H), 8.37 (dd, *J* = 2.2, 8.8 Hz, 1H), 8.23 (d, *J* = 7.7 Hz, 1H), 8.12 (d, *J* = 8.6 Hz, 2H), 7.74–7.67 (m, 2H), 7.57 (t, *J* = 7.9 Hz, 1H), 7.49 (t, *J* = 8.1 Hz, 1H), 7.33 (t, *J* = 7.7 Hz, 1H), 7.19 (d, *J* = 8.6 Hz, 2H), 7.07 (dd, *J* = 1.7, 8.4 Hz, 1H), 6.93–6.85 (m, 2H), 3.94 (s, 3H), 3.86 (s, 3H), 2.27 (s, 3H); ^{13}C NMR (100 MHz, DMSO–d_6) δ: 163.6, 160.7, 159.9, 154.1, 153.3, 143.4, 141.5, 140.7, 138.9, 136.8, 134.2, 130.6, 130.2, 129.7, 129.6, 129.5, 128.5, 127.5, 127.0, 125.9, 122.0, 121.1, 120.9, 120.4, 120.2, 115.9, 114.1, 113.2, 112.6, 112.4, 55.7, 55.3, 22.9; MS (ESI): *m/z* 582 [M + H]$^+$; HRM (ESI): *m/z* calcd for $C_{35}H_{28}O_4N_5$: 582.21358; found: 582.21445 [M + H]$^+$.

1-(4-Methoxyphenyl)-*N*-(3-(4-methoxyphenyl)-2-methyl-4-oxo-3,4-dihydroquinazolin-6-yl)-9*H*-pyrido[3,4-*b*]indole-3-carboxamide (10c): White solid; Yield: 90%; Mp: 326–328 °C; ^{1}H NMR (300 MHz, $CDCl_3$ + DMSO–d_6) δ: 11.57 (s, 1H), 10.63 (s, 1H), 8.90 (s, 1H), 8.61 (d, *J* = 3.0 Hz, 1H), 8.34 (dd, *J* = 2.4, 8.6Hz, 1H), 8.24 (d, *J* = 7.9 Hz, 1H), 8.13 (d, *J* = 8.4 Hz, 2H), 7.71 (d, *J* = 2.8 Hz, 1H), 7.6 (d, *J* = 3.5 Hz, 1H), 7.57 (t, *J* = 7.3 Hz, 1H), 7.33 (t, *J* = 7.4 Hz, 1H), 7.24 (d, *J* = 8.6 Hz, 2H), 7.19 (d, *J* = 8.6 Hz, 2H), 7.08 (d, *J* = 8.6 Hz, 2H), 3.95 (s, 3H), 3.89 (s, 3H), 2.24 (s, 3H); ^{13}C NMR (75 MHz, $CDCl_3$ + DMSO–d_6) δ: 163.2, 161.2, 159.7, 159.1, 152.9, 143.2, 141.4, 140.5, 138.6, 136.5, 134.2, 133.0, 130.1, 129.9, 129.6, 128.9, 128.0, 126.8, 124.2, 121.3, 121.0, 120.5, 119.8, 115.6, 114.4, 113.8, 112.6, 112.4, 55.1, 55.0, 23.6; MS (ESI): *m/z* 582 [M + H]$^+$; HRMS (ESI): *m/z* calcd for $C_{35}H_{28}O_4N_5$: 582.21358; found: 582.21413 [M + H]$^+$.

1-(4-Methoxyphenyl)-*N*-(2-methyl-4-oxo-3-(*m*-tolyl)-3,4-dihydroquinazolin-6-yl)-9*H*-pyrido[3,4-*b*]indole-3-carboxamide (10d): Off white solid; Yield: 88%; Mp: 300–302 °C; ^{1}H NMR (300 MHz, $CDCl_3$ + DMSO–d_6) δ: 11.92 (s, 1H), 10.79 (s, 1H), 8.95 (s, 1H), 8.77 (d, *J* =2.4 Hz, 1H), 8.46 (d, *J* =7.9 Hz, 1H), 8.33(dd, *J* = 2.4, 8.6 Hz, 1H), 8.25 (d, *J* = 8.8 Hz, 2H), 7.73 (d, *J* = 4.4 Hz, 1H), 7.70 (d, *J* = 4.9 Hz, 1H), 7.62 (t, *J* = 7.9 Hz, 1H), 7.47 (t, *J* = 7.7 Hz, 1H), 7.35 (d, *J* = 6.8 Hz, 2H), 7.29–7.22 (m, 4H), 3.91 (s, 3H), 2.40 (s, 3H), 2.14 (s, 3H); ^{13}C NMR (75 MHz, $CDCl_3$ + DMSO–d_6) δ: 163.5, 161.1, 159.9, 152.8, 143.3, 141.4, 140.6, 139.0, 138.9, 137.7, 136.7, 134.2, 130.1, 129.7, 129.6, 129.4, 129.2, 128.6, 128.4, 127.3, 126.9, 125.2, 121.8, 121.1, 120.5, 120.1, 115.8, 114.0, 113.1, 112.6, 55.2, 23.7, 20.7; MS (ESI): *m/z* 566 [M + H]$^+$; HRM (ESI): *m/z* calcd for $C_{35}H_{28}O_3N_5$: 566.21867; found: 566.21700 [M+ H]$^+$.

N-(3-(3-Chlorophenyl)-2-methyl-4-oxo-3,4-dihydroquinazolin-6-yl)-1-(4-methoxyphenyl)-9H-pyrido[3,4-b]indole-3-carboxamide (10e): Pale yellow solid; Yield: 85%; Mp: 306–308 °C; 1H NMR (300 MHz, CDCl3 + DMSO d6) δ: 11.92 (s, 1H), 10.80 (s, 1H), 8.95 (s, 1H), 8.78 (d, J = 2.4 Hz, 1H), 8.45 (d, J = 7. Hz, 1H), 8.34 (dd, J = 2.2, 8.8 Hz, 1H), 8.25 (d, J = 8.8 Hz, 2H), 7.76–7.68 (m, 3H) 7.66–7.58 (m, 3H), 7.55–7.47 (m, 1H), 7.34 (d, J = 7.4 Hz, 1H), 7.24 (d, J = 8.8 Hz, 2H) 3.91 (s, 3H), 2.15 (s, 3H); 13C NMR (125 MHz, DMSO–d6) δ: 163.7, 161.2, 160.0, 152.5, 143.4, 141.5, 140.8, 139.3, 139.0, 136.9, 134.2, 133.5, 131.1, 130.3, 129.8, 129.7, 129.0, 128.7, 128.6, 127.5, 127.4, 127.1, 122.0, 121.1, 120.6, 120.2, 115.9, 114.1, 113.2, 112.7, 55.3, 23.8; MS (ESI): m/z 586 [M + H]+; HRMS (ESI): m/z calcd for C34H25O3N5Cl: 586.16404; found: 586.16247 [M + H]+.

1-(4-Methoxyphenyl)-*N*-(2-methyl-4-oxo-3-(3-(trifluoromethyl)phenyl)-3,4-dihydroquinazolin-6-yl)-9*H*-pyrido[3,4-*b*]indole-3-carboxamide (10f): Pale yellow solid; Yield: 83%; Mp: 318–320 °C; ^{1}H NMR (300 MHz, $CDCl_3$ + DMSO–d_6) δ: 11.93 (s, 1H), 10.80 (s, 1H), 8.95 (s, 1H), 8.79 (d, *J* = 2.5 Hz, 1H), 8.45 (d, *J* = 8.0 Hz, 1H), 8.34 (dd, *J* = 2.5, 8.8 Hz, 1H), 8.24 (d, *J* = 8.8 Hz, 2H), 8.04 (s, 1H), 7.95–7.90 (m, 1H), 7.88–7.82 (m, 2H), 7.22 (d, *J* = 8.8 Hz, 2H), 7.61 (t, *J* = 7.9 Hz, 1H), 7.33 (t, *J* = 7.4 Hz, 1H), 7.23 (d, *J* = 8.8 Hz, 2H), 3.91 (s, 3H), 2.13 (s, 3H); ^{13}C NMR (100MHz, DMSO–d_6) δ: 163.7, 161.3, 152.4, 143.4, 141.5, 140.7, 139.0, 138.7, 136.9, 134.2, 130.0, 130.7, 130.2, 130.1, 129.7, 129.6, 128.5, 127.5, 127.1, 125.5, 125.0, 122.3, 122.0, 121.1, 120.5, 120.2, 115.9, 114.1, 113.2, 112.6, 130.4, 55.3, 23.9; MS (ESI): *m/z* 620 [M + H]$^+$; HRMS (ESI): *m/z* calcd for $C_{35}H_{25}O_3N_5F_3$: 620.19040; found: 620.19124 [M + H]$^+$.

1-(4-Methoxyphenyl)-*N*-(2-methyl-4-oxo-3-(3,4,5-trimethoxyphenyl)-3,4-dihydroquinazolin-6-yl)-9*H*-pyrido[3,4-*b*]indole-3-carboxamide (10g): Pale yellow solid; Yield: 76%; Mp: 197–198 °C; ^{1}H NMR (300 MHz, $CDCl_3$) δ: 10.51 (s, 1H), 8.99 (s, 1H), 8.97 (s, 1H), 8.65 (dd, *J* = 2.4,8.9 Hz, 1H), 8.27 (d, *J* = 2.4 Hz, 1H), 8.24 (d, *J* = 7.9 Hz, 1H), 8.01–7.97 (m, 2H), 7.75 (d, *J* = 8.9 Hz, 1H), 7.63–7.51 (m, 2H), 7.38 (t, *J* = 7.5 Hz,1H), 7.15–7.11 (m, 2H), 6.5 2 (s, 2H), 3.93 (s, 3H), 3.90 (s, 3H), 3.88 (s, 6H), 2.33 (s, 3H); ^{13}C NMR (75 MHz, DMSO–d_6) δ: 163.6, 161.1, 159.9, 153.2, 143.4, 141.5, 140.7, 139.0, 137.3, 136.7, 134.1, 133.5, 130.2, 129.7, 129.6, 128.5, 127.4, 126.9, 121.9, 121.1, 120.6, 120.2, 115.9, 114.1, 113.1, 112.6, 106.0, 59.9, 56.0, 55.2, 23.4; MS

(ESI): *m/z* 642 [M + H]$^+$; HRMS (ESI): *m/z* calcd for $C_{37}H_{32}O_6N_5$: 642.23471; found: 642.23370 [M + H]$^+$.

N-(3-(2-Methoxyphenyl)-2-methyl-4-oxo-3,4-dihydroquinazolin-6-yl)-1-(p-tolyl)-9H-pyrido[3,4-b]indole-3-carboxamide (10h): Pale yellow solid; Yield: 86%; Mp: 302–304°C; ^{1}H NMR (300 MHz, $CDCl_3$ + DMSO– d_6) δ: 11.34 (s, 1H) 10.60 (s, 1H), 8.94 (s, 1H), 8.49 (d, *J* = 2.1 Hz, 1H), 8.43 (dd, *J* = 2.3,8.7 Hz, 1H), 8.23 (d, *J* = 7.7 Hz, 1H), 8.03 (d, *J* = 8.1 Hz, 2H), 7.71 (t, *J* = 8.9 Hz, 2H), 7.61–7.50 (m, 2H), 7.46 (d, *J* = 7.9 Hz, 2H), 7.34 (t, *J* = 7.4 Hz,1H), 7.25 (dd, *J* = 1.5, 7.9 Hz, 1H), 7.15 (dd, *J* = 4.1,6.8 Hz, 2H), 3.83 (s, 3H), 2.51 (s, 3H), 2.22 (s, 3H); ^{13}C NMR (125 MHz, $CDCl_3$ + DMSO–d_6) δ: 163.2, 160.6, 153.9, 152.9, 143.3, 141.4, 140.7, 138.6, 138.2, 136.5, 134.4, 130.4, 130.3, 129.7, 129.1, 129.0, 128.5, 128.1, 126.9, 126.8, 125.8, 121.4, 120.9, 120.7, 120.4, 119.9, 115.7, 112.9, 112.4, 112.0, 55.4, 22.7, 20.8; MS (ESI): *m/z* 566 [M + H]$^+$; HRMS (ESI): *m/z* calcd for $C_{35}H_{28}O_3N_5$: 566.21867; found: 566.21894 [M + H]$^+$.

N-(3-(3-Methoxyphenyl)-2-methyl-4-oxo-3,4-dihydroquinazolin-6-yl)-1-(p-tolyl)-9H-pyrido[3,4-b]indole-3-carboxamide (10i): Pale yellow solid; Yield: 87%; Mp: 399–301°C; 1H NMR (300 MHz, CDCl3 + DMSO– d6) δ: 10.69 (s, 1H) 8.90 (s, 1H), 8.73 (d, J = 2.3 Hz, 1H), 8.32 (d, J = 7.9 Hz, 1H), 8.27 (dd, J = 2.3, 8.7 Hz, 1H), 8.14 (s, 1H), 8.10 (d, J = 7.9 Hz, 2H), 7.67 (d, J = 8.3 Hz, 1H),7.64 (d, J = 8.9 Hz, 1H), 7.55 (t, J = 7.5 Hz, 1H), 7.48–7.42 (m, 3H), 7.29 (t, J = 7.5 Hz, 1H), 7.05 (dd, J = 1.9, 8.1 Hz, 1H), 7.00 (t, J = 1.8 Hz, 1H), 6.94 (d, J = 8.3 Hz, 1H3.81 (s, 3H), 2.47 (s, 3H), 2.18 (s, 3H); 13C NMR (125 MHz, CDCl3 + DMSO–d6) δ: 163.5, 160.4, 160.0, 158.3, 157.8, 141.5, 140.8, 138.7, 138.4, 138.1, 137.3, 134.3, 130.2, 129.7, 129.1, 128.6, 128.4, 127.5, 125.2, 125.1, 121.8, 121.7, 121.0, 120.2, 120.0, 116.0, 114.7, 113.8, 113.4, 112.5, 55.2, 22.7, 20.8; MS (ESI): m/z 566 [M + H]+; HRMS (ESI): m/z calcd for C35H28O3N5: 566.21867; found: 566.21957 [M + H]+.

N-(3-(4-Methoxyphenyl)-2-methyl-4-oxo-3,4-dihydroquinazolin-6-yl)-1-(p-tolyl)-9H-pyrido[3,4-b]indole-3-carboxamide (10j): Off white solid; Yield: 89%; Mp: 322–324 °C; 1H NMR (300 MHz, CDCl3 + DMSO–d6) δ: 11.47 (s, 1H) 10.60 (s, 1H), 8.93 (s, 1H), 8.55 (s, 1H), 8.36 (d, J = 8.9 Hz, 1H), 8.23 (d, J = 7.9 Hz, 1H), 8.04 (d, J = 7.7 Hz, 2H), 7.70–7.64 (m, 2H), 7.57 (t, J = 7.5 Hz,1H), 7.47 (d, J = 7.9 Hz, 2H), 7.33 (t, J = 7.5 Hz, 1H), 7.23 (d, J = 8.9 Hz, 2H),7.08 (d, J = 8.9 Hz, 2H), 3.89 (s, 3H), 2.52 (s, 3H), 2.25 (s, 3H); 13C NMR (125 MHz, DMSO–d6) δ: 163.6, 161.4, 159.2, 153.4, 143.5, 141.6, 140.9, 139.1, 138.6, 136.7, 134.5, 134.4, 130.4, 129.8, 129.4, 129.3, 128.9, 128.7, 128.6, 126.9, 122.1, 121.1, 120.6, 120.3, 116.1, 114.6, 113.4, 112.7, 55.3, 23.9, 20.9, ; MS (ESI): m/z 566 [M + H]+; HRMS (ESI): m/z calcd for C35H28O3N5: 566.21867; found: 566.21892 [M + H]+.

N-(2-Methyl-4-oxo-3-(m-tolyl)-3,4-dihydroquinazolin-6-yl)-1-(p-tolyl)-9H- pyrido[3,4-b]indole-3-carboxamide (10k): Off white solid; Yield: 85%; Mp: 324–326 °C; 1H NMR (300 MHz, CDCl3 + DMSO–d6) δ: 10.76 (s, 1H) 8.95 (s, 1H), 8.76 (d, J = 2.3 Hz, 1H), 8.42 (d, J = 7.9 Hz, 1H), 8.31(dd, J = 2.3, 8.7 Hz, 1H), 8.15(d, J = 7.9 Hz, 2H), 7.69 (t, J = 8.3 Hz, 2H), 7.59 (t, J = 7.4 Hz, 1H), 7.51–7.42 (m, 3H), 7.36–7.29 (m, 2H), 7.27–7.20 (m, 2H), 2.48 (s, 3H), 2.40 (s, 3H), 2.14 (s, 3H); 13C NMR (75 MHz, DMSO–d6) δ: 163.5, 161.1, 152.8, 143.4, 141.5, 140.8, 139.0, 138.4, 137.8, 136.8, 136.7, 134.4, 134.3, 129.8, 129.4, 129.2, 128.7, 128.6, 128.5, 127.3, 126.9, 125.2, 121.9, 121.8, 121.0, 120.5, 120.1, 115.8, 113.4, 112.6, 23.7, 20.8, 20.7; MS (ESI): m/z 550 [M + H]+; HRMS (ESI): m/z calcd for C35H28O3N5: 550.22375; found: 550.22164 [M + H]+.

N-(3-(3-Chlorophenyl)-2-methyl-4-oxo-3,4-dihydroquinazolin-6-yl)-1-(p-tolyl)-9H-pyrido[3,4-b]indole-3-carboxamide (10l): Off white solid; Yield: 84%; Mp: 240–242 °C; 1H NMR (300 MHz, CDCl3 + DMSO–d6) δ: 11.56 (s, 1H), 10.64 (s, 1H) 8.93 (s, 1H), 8.61 (d, J = 2.4 Hz, 1H), 8.35 (dd, J = 2.4, 8.8 Hz, 1H), 8.24 (d, J = 7.7 Hz, 1H), 8.02 (d, J = 7.9 Hz, 2H), 7.72–7.68 (m, 2H), 7.61– 7.53 (m, 3H), 7.48 (d, J = 7.9 Hz, 2H), 7.41 (t, J = 1.5 Hz, 1H), 7.35 (d, J = 7.7 Hz, 1H), 7.32–7.27 (m, 1H), 2.52 (s, 3H), 2.26 (s, 3H); 13C NMR (75 MHz, DMSO–d6) δ: 163.1, 160.9, 151.7, 143.0, 141.3, 140.6, 138.8, 138.5, 138.1, 136.6, 134.3, 133.9, 130.5, 129.6, 128.9, 128.7, 128.3, 128.2, 128.1, 128.0, 126.8, 126.7, 121.2, 121.1, 120.9, 120.3, 119.8, 115.4, 112.8, 112.3, 23.5, 20.7; MS (ESI): *m/z* 570 [M + H]$^+$; HRMS (ESI): *m/z* calcd for $C_{35}H_{24}O_2N_5Cl$: 570.16913; found: 570.16743 [M + H]$^+$.

N-(2-methyl-4-oxo-3-(3-(trifluoromethyl)phenyl)-3,4-dihydroquinazolin-6-yl)-1-(p-tolyl)-9H-pyrido[3,4-b]indole-3-carboxamide (10m): Off white solid; Yield: 82%; Mp: 262–264 °C; 1H NMR (300 MHz, DMSO–d6) δ: 10.81 (s, 1H), 8.98 (s, 1H), 8.80 (d, J = 2.4 Hz, 1H), 8.47 (d, J = 7.9 Hz, 1H), 8.34 (dd, J = 2.4, 8.8 Hz, 1H), 8.17 (d, J = 7.9 Hz, 2H), 8.04 (s, 1H), 7.96–7.91 (m, 1H), 7.88–7.83 (m, 2H), 7.72 (d, J = 9.0 Hz, 2H), 7.62 (t, J = 7.3 Hz, 1H), 7.50 (d, J = 8.1 Hz, 2H), 7.34 (t, J = 7.5 Hz, 1H), 2.48 (s 3H), 2.13 (s, 3H); 13C NMR (75 MHz, DMSO–d6) δ: 163.6, 161.2, 152.3, 143.4, 141.5, 140.8, 139.0, 138.7, 138.5, 136.8, 134.8 and 134.3 (d, J = 3.8), 132.9, 130.7, 130.4, 130.0, 129.8, 129.8, 128.7, 128.5, 127.5, 127.0, 125.75 and 125.72 (d, J = 3.3), 125.4, 121.9, 121.8, 121.0, 120.5, 120.2, 115.8, 113.4, 112.6, 23.8, 20.8; MS (ESI): m/z 604 [M + H]+; HRMS (ESI): m/z calcd for C35H25O2N5F3: 604.19549; found: 604.19633 [M + H]+.

N-(2-Methyl-4-oxo-3-(3,4,5-trimethoxyphenyl)-3,4-dihydroquinazolin-6-yl)-1-(p-tolyl)-9H-pyrido[3,4-b]indole-3-carboxamide (10n): Off white solid; Yield: 90%; Mp: 303–305 °C; 1H NMR (300 MHz, CDCl3 + DMSO–d6) δ: 11.92 (s, 1H), 10.78 (s, 1H) 8.98 (s, 1H), 8.79 (d, J = 2.2 Hz, 1H), 8.46 (d, J = 7.9 Hz, 1 8.31(dd, J = 2.2, 8.8 Hz, 1H), 8.17 (d, J = 7.9 Hz, 2H), 773 (d, J = 4.1 Hz, 1H), 7.70 (d, J = 4.6 Hz, 1H), 7.62 (t, J = 7.4 Hz, 1H), 7.50 (d, J = 7.9 Hz, 2H), 7.34 (t, J = 7.7 Hz, 1H), 6.87(s, 2H), 3.79 (s, 6H), 3.76 (s, 3H), 2.50 (s, 3H), 2.23 (s, 3H); 13C NMR (7z MHz, DMSO–d6) δ: 163.6, 161.3, 161.1, 153.3, 143.4, 141.5, 140.9, 139.1, 138.6, 137.4, 136.7, 134.4, 134.3, 133.5, 129.8, 129.3, 128.7, 128.6, 127.5, 126.9, 122.0, 121.0, 120.6, 120.2, 116.0, 113.5, 112.7, 106.0, 60.0, 56.1, 23.5, 21.0; MS (ESI): m/z 626 [M + H]+; HRMS (ESI): m/z calcd for C37H32O5N5: 626.23739; found: 626.23838 [M + H]+.

1-(4-Fluorophenyl)-*N*-(3-(2-methoxyphenyl)-2-methyl-4-oxo-3,4-dihydroquinazolin-6-yl)-9*H*-pyrido[3,4-*b*]indole-3-carboxamide (10o): Off white solid; Yield: 82%; Mp: 224–226 °C; 1H NMR (500 MHz, CDCl3 + DMSO–d6) δ: 11.71 (s, 1H), 10.61 (s, 1H), 8.93 (s, 1H), 8.67 (d, J = 2.4 Hz, 1H), 8.33–8.18 (m, 4H), 7.73–7.65 (m, 2H), 7.61–7.48 (m, 2H), 7.42–7.32 (m, 3H), 7.29 (dd, J = 1.5, 7.7 Hz, 1H), 7.20–7.11 (m, 2H), 3.83 (s, 3H), 2.19 (s,

3H); 13C NMR (75 MHz, CDCl3 + DMSO– d6) δ: 162.8, 160.8 160.7, 153.9, 152.9, 143.3, 141.4, 139.4, 138.4, 134.3, 133.4, 133.3, 130.4 and 130.3 (d, J = 8.8 Hz), 130.2, 129.9, 128.8, 128.1, 126.7, 126.5, 125.7, 121.0, 120.9, 120.6, 120.4, 119.8, 115.5, 115.2 and 115.0 (d, J = 21.4 Hz), 113.0, 112.2, 111.7, 55.2, 22.7; MS (ESI): m/z 570 [M + H]+; HRMS (ESI): m/z calcd for C34H25O3N5F: 570.19359; found: 570.19298 [M + H]+.

1-(4-Fluorophenyl)-*N*-(3-(3-methoxyphenyl)-2-methyl-4-oxo-3,4-dihydroquinazolin- 6-yl)-9*H*-pyrido[3,4-*b*]indole-3-carboxamide (10p): Pale yellow solid; Yield: 84%; Mp: 236–238 °C; ^{1}H NMR (300 MHz, $CDCl_3$ + DMSO– d_6) δ:11.71 (s, 1H), 10.62 (s, 1H) 8.92 (s, 1H), 8.68 (d, *J* = 2.4 Hz, 1H), 8.33–8.19 (m, 4H), 7.70 (d, *J* = 4.5 Hz, 1H), 7.67 (d, *J* = 4.9 Hz, 1H), 7.58 (t, *J* = 7.9 Hz, 1H), 7.49 (t, *J* = 8.3 Hz, 1H), 7.42–7.30 (m, 3H), 7. 07 (dd, *J* = 1.5, 8.6 Hz, 1H), 6.95–6.89 (m, 2H), 3.86 (s, 3H), 2.25 (s, 3H); ^{13}C NMR (75 MHz, $CDCl_3$ + DMSO–d_6) δ: 164.0 and 160.8 (d, *J* = 247.0 Hz), 163.1, 160.9, 159.9, 152.3, 143.2, 141.4, 139.5, 138.7, 138.6, 136.5, 134.2, 133.5, 133.4, 130.7 and 130.6 (d, *J* = 8.2 Hz), 129.9, 128.2, 126.9, 126.7, 121.3, 120.9, 120.4, 119.9, 115.6, 115.3 115.0, 114.3, 113.6, 113.2, 112.3, 55.0, 23.4; MS (ESI): *m/z* 570 [M + H]$^+$; HRMS (ESI): *m/z* calcd for $C_{34}H_{25}O_3N_5F$: 570.19359; found: 570.19323 [M + H]$^+$.

1-(4-Fluorophenyl)-N-(3-(4-methoxyphenyl)-2-methyl-4-oxo-3,4-dihydroquinazolin- 6-yl)-9H-pyrido[3,4-b]indole-3-carboxamide (10q): Pale yellow solid; Yield: 85%; Mp: 298–300 °C; 1H NMR (300 MHz, CDCl3 + DMSO– d6) δ: 11.52 (s, 1H), 10.55 (s, 1H) 8.95 (s, 1H), 8.55 (d, J = 2.4 Hz, 1H), 8.38 (dd, J = 2.4, 8.8 Hz, 1H), 8.24 (d, J = 7.7 Hz, 1H), 8.20–8.13 (m, 2H), 7.71 (d, J = 4.9 Hz, 1H), 7.68 (d, J = 4.1 Hz, 1H), 7.58 (t, J = 7.1 Hz, 1H), 7.40–7.31 (m, 3H), 7.22 (d, J = 8.6 Hz 2H), 7.08 (d, J = 8.8 Hz, 2H), 3.89 (s, 3H), 2.25 (s, 3H); 13C NMR (75 MHz, CDCl3 + DMSO–d6) δ: 164.0 and 160.7 (d, J = 248.1 Hz), 162.8, 161.2, 159.1, 152.8, 143.3, 141.3, 139.4, 138.3, 136.2, 134.3, 133.4, 133.3, 130.4 and 130.3 (d, J = 8.2 Hz), 130.2, 129.8, 128.6, 128.0, 126.7, 126.4, 125.7, 121.0, 120.9, 120.4, 119.8, 115.4, 115.2 and 115.0 (d, J = 21.4 Hz), 112.9, 54.9, 23.6; MS (ESI): m/z 570 [M + H]+; HRMS (ESI): m/z calcd for C34H25O3N5F: 570.19359; found: 570.19163 [M + H]+.

1-(4-Fluorophenyl)-*N*-(2-methyl-4-oxo-3-(*m*-tolyl)-3,4-dihydroquinazolin-6-yl)-9*H*-pyrido[3,4-*b*]indole-3-carboxamide (10r): Off white solid; Yield: 83%; Mp: 215–217 °C; 1H NMR (300 MHz, CDCl3 + DMSO–d6) δ: 11.71 (s, 1H), 10.62 (s, 1H) 8.93 (s, 1H), 8.68 (d, J = 2.2 Hz, 1H), 8.33–8.19 (m, 4H), 7.71 (d, J = 4.1 Hz, 1H), 7.68 (d, J = 4.7 Hz, 1H), 7.58 (t, J = 7.1 Hz, 1H), 7.47 (t, J = 4.7 Hz, 1H), 7.41–7.30 (m, 4H), 7.17–7.11 (m, 2H), 2.46 (s, 3H), 2.22 (s, 3H); 13C NMR (75 MHz, CDCl3 DMSO–d6) δ: 164.1 and 160.8 (d, J = 248.4), 163.3, 161.0, 152.6, 143.3 141.5, 139.6, 139.0 and 138.9 (d, J = 8.2 Hz), 137.6, 136.6, 134.3, 133.55, 133.52, 130.9 and 130.8 (d, J = 8.2 Hz), 129.9, 129.3, 129.1, 128.46, 128.41, 127.1, 126.8, 125.0, 121.6, 121.0, 120.5, 120.1, 115.8, 115.5 and 115.2 (d, J = 21.4 Hz), 113.4, 112.4, 23.6, 20.6; MS (ESI): m/z 554 [M + H]+; HRMS (ESI): m/z calcd for C34H25O2N5F: 554.19868; found: 554.19655 [M + H]+.

1-(4-Fluorophenyl)-*N*-(3-(3-chlorophenyl)-2-methyl-4-oxo-3,4-dihydroquinazolin-6- yl)-9*H*-pyrido[3,4-*b*]indole-3-carboxamide (10s): Pale yellow solid; Yield: 82%; Mp: 225–227 °C; 1H NMR (300 MHz, CDCl3 + DMSO–d6) δ: 11.75 (s, 1H), 10.65 (s, 1H), 8.93 (s, 1H), 8.71 (d, J = 2.0 Hz, 1H), 8.34–8.20 (m, 4H), 7.73–7.66 (m, 2H), 7.62–7.52 (m, 3H), 7.47 (s, 1H), 7.42–7.30 (m, 4H), 2.24 (s, 3H); 13C NMR (75 MHz, CDCl3 + DMSO–d6) δ: 164.1and 160.8 (d, J = 247.5 Hz) 163.3, 161.0, 152.1, 143.2, 141.5, 139.5, 139.0, 138.9, 136.7, 134.3, 133.7, 133.5, 130.9, 130.88, and 130.83, (d, J = 3.8 Hz), 129.9, 128.9, 128.5, 128.4, 127.2, 127.1, 126.8, 121.6, 121.0, 120.4, 120.1, 115.8, 115.5 and 115.2 (d, J = 22.0 Hz), 113.5, 112.4, 23.6; MS (ESI): m/z 574 [M + H]+; HRMS (ESI): m/z calcd for C33H22O2N5ClF: 574.14406; found: 574.14220 [M + H]+.

1-(4-Fluorophenyl)-N-(2-methyl-4-oxo-3-(3-(trifluoromethyl)phenyl)-3,4- dihydroquinazolin-6-yl)-9*H*-pyrido[3,4-*b*]indole-3-carboxamide (10t): Off white solid; Yield: 80%; Mp: 232–234 °C; 1H NMR (300 MHz, CDCl3 + DMSO–d6) δ: 10.74 (s, 1H) 8.95 (s, 1H), 8.78 (d, J = 2.2 Hz, 1H), 8.39–8.27 (m, 4H), 7.92–7.76 (m, 4H), 7.70 (t, J = 6.4 Hz, 2H), 7.59 (t, J = 7.9 Hz, 1H), 7.44 (t, J = 8.4 Hz, 2H), 7.33 (t, J = 7.5 Hz, 1H), 2.17 (s, 3H); 13C NMR (75 MHz, CDCl3 + DMSO–d6) δ: 164.0 and 160.8 (d, J = 247.0 Hz), 163.1, 161.0, 151.7, 143.1, 141.4, 139.5, 138.6, 138.3, 136.6, 134.3, 133.47, and 133.44, (d, J = 2.2 Hz), 132.2, 130.9, 130.7, and 130.6, (d, J = 8.2 Hz), 130.5, 130.3, 129.9, 128.2, 127.0, 126.8, 125.3 (dd, J = 3.3, 15.4 Hz), 124.9, 121.3, 120.9, 120.3, 119.9, 115.6, 115.3 and 115.0 (d, J = 21.4 Hz), 113.2, 112.3, 23.6; MS (ESI): m/z 608 [M + H]+; HRMS (ESI): m/z calcd for C34H22O2N5F4: 608.17041; found: 608.16913 [M + H]+.

1-(4-Fluorophenyl)-*N*-(2-methyl-4-oxo-3-(3,4,5-trimethoxyphenyl)-3,4-dihydroquinazolin-6-yl)-9*H*-pyrido[3,4-*b*]indole-3-carboxamide (10u): Off white solid; Yield: 86%; Mp: 284–286 °C; ^{1}H NMR (300 MHz, $CDCl_3$ + DMSO–d_6) δ: 11.29 (bs, 1H), 10.54 (bs, 1H) 8.98 (bs, 1H), 8.52–8.46 (m, 2H), 8.24 (d, *J* = 7.4 Hz, 1H), 8.17–8.11 (m, 2H), 7.74 (d, *J* = 8.5 Hz, 1H), 7.68 (d, *J* = 8.3 Hz, 1H), 7.59 (t, *J* = 7.0 Hz, 1H), 7.46 (d, *J* = 1.3 Hz, 1H), 7.39–7.32 (m, 2H), 6.56 (s, 2H), 3.92 (s, 3H), 3.89 (s, 6H), 2.34 (s, 3H); ^{13}C NMR (75 MHz, $CDCl_3$ + DMSO–d_6) δ: 163.1, 161.0, 160.8, 153.2, 152.8, 143.2, 141.4, 139.4, 138.7, 137.3, 136.5, 134.2, 133.4, 133.2, 130.9, 130.7 and 130.6, (d, *J* = 7.7 Hz), 128.2, 126.9, 126.7, 121.4, 120.9, 120.5, 119.9, 115.6, 115.3 and 115.0 (d, *J* = 20.9 Hz), 113.2, 112.3, 105.5, 59.8, 55.8, 23.3; MS (ESI): *m/z* 630 [M + H]$^+$; HRMS (ESI): *m/z* calcd fo $C_{36}H_{29}O_5N_5F$: 630.21472; found: 630.21350 [M + H]$^+$.

N-(3-(2-Methoxyphenyl)-2-methyl-4-oxo-3,4-dihydroquinazolin-6-yl)-1-(3,4,5-trimethoxyphenyl)-9H-pyrido[3,4-b]indole-3-carboxamide (10v): Off white solid; Yield: 89%; Mp: 223–225 °C; 1H NMR (300 MHz, CDCl3) δ: 11.67 (s, 1H), 10.59 (s, 1H) 8.95 (s, 1H), 8.56 (d, J = 2.4 Hz, 1H), 8.37 (dd, J = 2.4, 8.6 Hz, 1H), 8.25 (d, J = 7.7 Hz, 1H), 7.72 (d, J = 3.5 Hz, 1H), 7.69 (d, J = 2.8 Hz, 1H), 7.59 (d, J 7.1 Hz, 1H), 7.56–7.48 (m, 1H), 7.38–7.30 (m, 3H), 7. 26 (dd, J = 1.8, 8.1 Hz, 1H), 7.18–7.11 (m, 2H), 4.05 (s, 6H), 3.95 (s, 3H), 3.83 (s, 3H), 2.21 (s, 3H); 13C NMR (75 MHz, DMSO-d6) δ: 163.5, 160.6,154.1, 153.3, 153.0, 143.4, 141.4, 141.0, 138.9, 138.2, 136.8, 134.4, 132.6, 130.6, 129.7, 129.5, 128.6, 127.4, 127.0, 125.9, 122.0, 121.1, 120.9, 120.4, 120.2, 115.8, 113.6, 112.6, 112.4, 106.3, 59.9, 55.9, 55.7, 22.9; MS (ESI): m/z 642 [M + H]+; HRMS (ESI): m/z calcd for C37H32O6N5 642.23471; found: 642.23459 [M + H]+.

N-(3-(3-Methoxyphenyl)-2-methyl-4-oxo-3,4-dihydroquinazolin-6-yl)-1-(3,4,5-trimethoxyphenyl)-9H-pyrido[3,4-b]indole-3-carboxamide (10w): Yellow solid;

Yield: 90%; Mp: 217–219 °C; 1H NMR (300 MHz, CDCl3) δ: 10.46 (s, 1H) 9.10(s,1H), 8.98 (s, 1H), 8.60 (dd, J = 3.0,9.0 Hz, 1H), 8.30 (d, J = 3.0 Hz, 1H), 8.23 (d, J = 8.3 Hz, 1H), 7.74 (d, J = 8.3 Hz, 1H), 7.60 (dd, J = 7.5,15.1 Hz, 2H), 7.47–7.35 (m, 2H), 7.17 (s, 2H), 7.02 (dd, J = 2.2, 8.3 Hz, 1H), 6.85 (d, J = 9.0 Hz, 1H), 6.81 (t, J = 4.5 Hz, 1H), 3.97 (s, 6H), 3.94 (s, 3H), 3.83 (s, 3H), 2.27 (s, 3H); 13C NMR (75 MHz, CDCl3 + DMSO-d6) δ: 163.0, 161.2, 160.1, 153.0, 152.3, 143.1, 141.3, 140.6, 138.3, 138.2, 138.1,136.4, 134.6, 132.8, 130.1, 129.8, 128.0, 127.1,126.2, 121.1, 121.0, 120.5, 119.9, 119.5, 115.2, 114.3, 113.3, 113.1, 112.2, 105.4, 60.3, 55.8, 54.9, 23.4; MS (ESI): m/z 642 [M + H]+; HRMS (ESI): m/z calcd for C37H32O6N5: 642.23471; found: 642.23426 [M + H]+.

N-(3-(4-Methoxyphenyl)-2-methyl-4-oxo-3,4-dihydroquinazolin-6-yl)-1-(3,4,5-trimethoxyphenyl)-9H-pyrido[3,4-b]indole-3-carboxamide (10x): Pale yellow solid; Yield: 91%; Mp: 202–204 °C; ^{1}H NMR (500 MHz, $CDCl_3$) δ: 10.46 (s, 1H) 9.02 (s, 1H), 8.98 (s, 1H), 8.60 (dd, *J* = 2.4,8.8 Hz, 1H), 8.29 (d, *J* = 2.4 Hz, 1H), 8.24 (d, *J* = 7.9 Hz, 1H), 7.74 (d, *J* = 8.8 Hz, 1H), 7.61 (t, *J* = 8.1 Hz, 1H),7.56 (d, *J* = 8.1 Hz, 1H), 7.39 (t, *J* = 7.9 Hz,1H),7.19–7.15 (m, 4H), 7.05–7.01 (m, 2H), 3.97 (s, 6H), 3.95 (s, 3H), 3.86 (s, 3H), 2.25 (s, 3H); ^{13}C NMR (75 MHz, DMSO–d_6) δ: 163.5, 161.3, 159.1, 153.4, 153.0, 143.4, 141.4, 141.0, 138.9, 138.2, 136.7, 134.4, 132.6, 130.3, 129.7, 129.4, 128.6, 127.2, 126.9, 122.0, 121.1, 120.6, 120.2, 115.7, 114.5, 113.5, 112.6, 106.3, 59.9, 55.9, 55.3, 23.8; MS (ESI): *m/z* 642 [M + H]$^+$; HRMS (ESI): *m/z* calcd for $C_{37}H_{32}O_6N_5$: 642.23471; found: 642.23442 [M + H]$^+$.

N-(2-Methyl-4-oxo-3-(m-tolyl)-3,4-dihydroquinazolin-6-yl)-1-(3,4,5- trimethoxyphenyl)-9H-pyrido[3,4-b]indole-3-carboxamide (10y): Pale yellow solid; Yield: 89%; Mp: 198–200 °C; 1H NMR (300 MHz, CDCl3) δ: 10.46 (s, 1H) 9.08 (s, 1H), 8.99 (s, 1H), 8.62 (dd, J = 2.2, 9.0 Hz, 1H), 8.29 (d, J = 2.2 Hz, 1H), 8.24 (d, J = 7.5 Hz, 1H), 7.75 (d, J = 9.0 Hz, 1H), 7.65–7.54 (m, 2H), 7.45–7.35 (m, 2H), 7.30 (s, 1H), 7.17 (s, 2H), 7.10–7.03 (m, 2H), 3.97 (s, 6H), 3.94 (s, 3H), 2.41(s, 3H), 2.24 (s, 3H); 13C NMR (7 MHz, DMSO–d6) δ; 163.5, 161.1, 153.0, 152.8, 143.3, 141.4, 141.0, 139.0, 138.9, 138.2, 137.7, 136.7, 134.4, 132.6, 129.7, 129.4, 129.2, 128.6, 128.5, 127.3, 127.0, 125.2, 122.0, 121.120.5, 120.2, 115.7, 113.5, 112.6, 106.3, 59.9, 55.9, 23.7, 20.7; MS (ESI): m/z 626 [M + H]+; HRMS (ESI): m/z calcd for C37H32O5N5: 626.23980; found: 626.23901 [M + H]+.

N-(3-(3-Chlorophenyl)-2-methyl-4-oxo-3,4-dihydroquinazolin-6-yl)-1-(3,4,5-trimethoxyphenyl)-9H-pyrido[3,4-b]indole-3-carboxamide (10z): Off white solid; Yield: 88%; Mp: 214–216 °C; 1H NMR (300 MHz, CDCl3) δ: 10.48 (s, 1H) 9.01 (s, 1H), 8.86 (s, 1H), 8.63 (dd, J = 2.6,8.9 Hz, 1H), 8.31 (d, J = 2.4 Hz, 1H), 8.27 (d, J = 7.7 Hz, 1H), 7.76 (d, J = 8.9 Hz, 1H),7.63–7.58 (m, 2H), 7.53–7.50 (m, 2H), 7.40 (t, J = 7.9 Hz, 1H), 7.33 (s, 1H), 7.22–7.18 (m, 1H), 7.16 (s, 2H), 3.99 (s, 6H), 3.97 (s, 3H), 2.27 (s, 3H); 13C NMR (125 MHz, DMSO–d6) δ; 163.5, 161.1, 153.0, 152.4, 143.3, 141.4, 141.0, 139.2, 138.9, 138.2, 136.8, 134.5, 134.4, 133.5, 132.6, 131.0, 129.7, 129.0, 128.6, 127.4, 127.0, 122.0, 121.1, 120.5, 120.2, 115.7, 113.5, 112.7, 112.6, 106.3, 59.9, 55.9, 23.7; MS (ESI): m/z 646 [M + H]+; HRMS (ESI): m/z calcd for C36H29O5N5Cl: 646.18517; found: 646.18419 [M + H]+.

N-(2-Methyl-4-oxo-3-(3-(trifluoromethyl)phenyl)-3,4-dihydroquinazolin-6-yl)-1-(3,4,5-trimethoxyphenyl)-9H-pyrido[3,4-b]indole-3-carboxamide (10aa): Off white solid; Yield: 85%; Mp: 204–206 °C; 1H NMR (300 MHz, CDCl3) δ: 10.46 (s, 1H) 9.01 (s, 1H), 8.97 (s, 1H), 8.59 (dd, J = 2.4,8.9 Hz, 1H), 8.31 (d, J = 2.4 Hz, 1H), 8.23 (d, J = 7. Hz, 1H), 7.81–7.69 (m, 3H), 7.62–7.57 (m, 3H), 7.51 (d, J = 7.4 Hz, 1H),. 7.39 (t, J = 7.9 Hz, 1H), 7.16 (s, 2H), 3.97 (s, 6H), 3.95 (s, 3H), 2.23 (s, 3H); 13C NMR (125 MHz, DMSO–d6) δ: 163.5, 161.2, 153.0, 152.3, 143.3, 141.5, 141.0, 138.9, 138.7, 138.2, 136.9, 134.4, 132.9, 132.6, 130.7, 130.4, 130.0, 129.7, 128.6, 127.4, 127.0, 125.7, 122.0, 121.8, 121.1, 120.5, 120.2, 115.7, 113.6, 112.6, 106.3, 59.9, 55.9, 23.8; MS (ESI): m/z 680 [M + H]+; HRMS (ESI): m/z calcd for C37H29O5N5F3: 680.21153; found: 680.21219 [M + H]+.

N-(2-Methyl-4-oxo-3-(3,4,5-trimethoxyphenyl)-3,4-dihydroquinazolin-6-yl)-1-(3,4,5- trimethoxyphenyl)-9H-pyrido[3,4-b]indole-3-carboxamide (10ab): Off white solid; Yield: 93% Mp: 218–220 °C; 1H NMR (300 MHz, CDCl3) δ: 10.48 (s, 1H) 9.02 (s, 1H), 8.86 (s, 1H), 8.63 (dd, J = 2.4,8.9 Hz, 1H), 8.32 (d, J = 2.3 Hz, 1H), 8.26 (d, J = 7.9 Hz, 1H), 7.76 (d, J = 8.9 Hz, 1H), 7.66–7.56 (m, 2H), 7.41 (t, J = 7.5Hz, 1H), 7.17 (s, 2H), 6.51 (s, 2H), 4.0 (s, 6H) 3.97(s, 3H), 3.92(s, 3H), 3.87 (s, 6H), 2.33 (s, 3H); 13C NMR (75 MHz, DMSO–d6) δ: 163.0, 161.0, 153.2, 152.8, 152.6, 143.0, 141.3, 140.6, 138.4, 138.0, 137.7, 137.4, 136.4, 134.4, 133.0, 132.5, 129.6, 128.0, 126.7, 126.6, 121.1, 120.9, 120.4, 119.8, 115.9 112.9, 112.3, 105.8, 105.2, 59.9, 59.8, 55.7, 23.2; MS (ESI): m/z 702 [M + H]+; HRMS (ESI): m/z calcd for C39H32O8N5: 702.25534; found: 702.25607 [M + H]+.

BIOLOGY

Cytotoxic activity

The cytotoxic activity of all the synthesized compounds was determined using MTT assay, (40) against a panel of four human cancer cell lines such as A549 (lung cancer), MCF-7 (breast cancer), DU-145 (prostate cancer), HeLa (cervical cancer) and NIH3T3 cells (mouse embryonic fibroblast cell line), which were procured from National Centre for Cell Science (NCCS, Pune, India).1×104 cells/well were seeded in 200 µl DMEM, supplemented with 10% FBS in each well of 96-well microculture plates and incubated in a CO2 incubator for 24 h at 37 °C. All the compounds are added to the cells at different concentrations with proper control for 48 h. After 48 h of incubation, 20 µl MTT (3-(4,5-dimethylthiazol-2-yl)-2,5-diphenyl tetrazolium bromide) (5 mg/ml) was added to each well and the plates were further incubated for 4 h. Then the supernatant from each well was carefully removed, formazan crystals were dissolved in 200 µl of DMSO and absorbance was recorded at 570 nm wavelength using spectrophotometer. The assay was carried out thrice and the mean values were considered.

Cell cycle assay

Flow cytometric analysis (FACS) was performed by using Becton Dickinson FACS Caliber to evaluate the distribution of the cells through the cell cycle phases. 1 × 10^5 A549 cells were incubated with derivatives **10a** and **10e** at 1 and 2 µM concentrations (at their IC_{50} concentration) for 48 h. Untreated and treated cells were harvested, washed with PBS, fixed in cold ethanol (70%) and stained with propidium iodide (Sigma

Aldrich). Cell cycle was performed by following the protocol described by (41)Cell cycle assay was carried out thrice and the mean values were considered.

Topoisomerase I inhibition

The topo I inhibitory activity was measured in a DNA cleavage assay as described previously. (42) The pBR 322 plasmid DNA was purchased from Sigma Aldrich, USA and 0.5 µg of DNA was incubated with 1 unit of topo I enzyme (Invitrogen) in 1X NEB buffer (50 mM potassium acetate, 20 mM Tris-acetate, 10 mM magnesium acetate, 1 mM DTT). Camptothecin was used as a positive control. Camptothecin and β-carboline conjugates **10a, 10e** and **10u** at 25 µM were added to the Topo I-DNA complex and incubated at 37 °C for 30 min, allowing the formation of the ternary enzyme-DNA-ligand complex. Then the enzyme was inactivated by increasing the temperature to 65 °C. After the incubation, the samples were resolved using 1% agarose gel electrophoresis enables the visualization of cleavage products. The pBR322 DNA with no ligand was considered as control.

UV-Vis studies

UV-visible spectroscopic titrations were performed using ABI Lambda 40 UV-Vis spectrophotometer (Foster City, USA) at 25 °C using 1 cm path length quartz cuvette. Stock solution of 1 mM of CT-DNA (calf thymus DNA, which can form perfect double-stranded DNA structure) was prepared in 100 mM *Tris*-HCl (pH 7.0). Later, stock solution of 1 mM of synthesized β-carboline derivatives (10a, 10b, and 10c) was prepared by dissolving them in 1:1 DMSO:Milli Q water. UV-visible absorption titrations were performed by adding 10 µM CT DNA solution in 100 mM *Tris*-HCl (pH 7.0) each time to the quartz cuvette containing about 10 µM derivative solution. Titrations were carried out until the complex absorption band remains at a fixed wavelength upon five successive additions of CT-DNA. Absorption spectra were recorded from 200 nm to 500 nm by using spectrophotometer.

Fluorescence studies

Fluorescence emission spectra were measured at 25 °C using a Hitachi F7000 spectrofluorimeter (Maryland, USA) using a 1 cm path length quartz cuvette. Throughout the fluorescence experiment, the concentration of the compounds **10a**, **10b** and **10c** was kept constant (10 µM) and titrated with increasing concentrations of CT-DNA (each addition with an increment of 10 µM CT-DNA). Fluorescence spectra were recorded after each addition of CT-DNA to the fluorescent cuvette. After each experiment, the quartz cuvette was thoroughly washed with distilled water and dilutes nitric acid (approximately 0.1 N, nitric acid) to remove traces of derivative binding to the walls of quartz cuvette. **10a**, **10e**, and **10u** derivatives were excited at 315 nm, 295 nm and 303 nm respectively and emission spectra for each titration were collected in the range from 310 nm to 370 nm. Each spectrum was recorded three times and the average of three scans was taken.

Circular dichroism studies

Circular dichroism (CD) experiments were carried out using JASCO 815 CD spectropolarimeter (Jasco, Tokyo, Japan). CD spectrum was recorded from 220 to 320 nm to find the confirmation of DNA after CT-DNA-derivatives (**10a**, **10b** and **10e**) interaction. For CD experiments, $10x10^{-6}$ M of CT-DNA was used. For characterizing derivative-CT-DNA interaction, CD spectra is recorded in 1:0, 1:1 and 1:2 molar ratio of CT DNA:derivatives (**10a**, **10b** and **10e**) respectively. In this experiment, the concentration of CT DNA was kept constant and the test conjugates were added at 1:1 and 1:2 ratios. CD titrations were performed in 100 mM *Tris*-HCl (pH 7.0) at 25 °C. Each CD spectrum was recorded thrice and the average of three scans was considered.

Viscosity studies

Viscosity experiments were conducted on Ostwald viscometer, immersed in a water bath maintained at 25 °C. Viscosity experiments were performed for each complex (15 µM), after mixing them with CT-DNA solution (150 µM). Before mixing DNA and complexes, viscosity measurements were performed with CT-DNA alone. Et Br-CT-DNA and Hoechst 33342-CT-DNA complexes were considered as control. Et-Br was considered to find the extent of intercalation of these compounds with CT-DNA and Hoechst 33342 is an indicator for external binding of these compounds with DNA. DNA solution was prepared in 100 mM *Tris*-HCl (pH 7.0). The graph was drawn by plotting $(\eta/\eta_o)^{1/3}$ versus complex/CT-DNA, where η is the viscosity of CT- DNA in the presence of complexes and η_o is the viscosity of CT-DNA alone. Viscosity values were calculated according to the protocol mentioned by (43).

Molecular docking studies

The protein structure of human DNA topo I (70 kDa) in complex with the indenoisoquinoline (PDB code: 1SC7, resolution 3.0 Å) (43) was obtained from the RCSB PDB and was prepared using the Protein Preparation Wizard of the Maeströ 9.9. In order to define the correct ionization and tautomeric states of amino acid residues, hydrogen atoms were added to the protein. The Prime module incorporated in Maeströ 9.9 was used to correct the missing side chains of residues. Further, OPLS- 2005 force field was used to diminish steric clashes that could possibly exist in the structures under study. The minimization was stopped when the energy converged or the Root Mean Square Deviation (RMSD) reached a maximum cut off of 0.30 Å. Water molecules beyond 5 Å from hetero groups were deleted. Molecular docking studies were performed using Glide, (41) keeping the grid box of size 12 Å from the centroid to cover the entire vicinity of active site.

CONCLUSION

In summary, we have synthesized a series of new quinazolinone linked β-carboline conjugates as DNA intercalative topo I inhibitors. These compounds displayed good cytotoxic activity, particularly in A549 cells as well as promising DNA binding affinity. Among all the tested compounds, **10a**, **10e** and **10u** showed significant cytotoxicity against tested cell lines with IC_{50} values are ranging from 01.19±0.33 to 5.37±0.28 µM. These active compounds showed good correlation between their topo I inhibitory activity and cytotoxicity toward tested cancer cell lines. Investigation of the structure-activity relationship studies indicated that the electron donating and halogen groups present

on both phenyl rings (R_1 and R_2) are important in enhancing both cytotoxic activity as well as enzyme inhibition. The cell cycle analysis showed that this class of compounds can significantly induce the cell cycle arrest in G2/M phase. In addition, the effect of these compounds on topo I was studied by unwinding assay and the results indicated that active compounds **10a**, **10e** and **10u** could significantly inhibit the activity of topo I. Furthermore, the DNA binding potentiality of these compounds has been evaluated through biophysical spectroscopic studies like UV-visible, fluorescence titration, and circular dichroism as well as with viscosity. All these studies revealed that these compounds interact well with DNA through intercalative mode of binding, which was further supported by molecular docking studies. In view of the fact that topo I is an important target for cancer chemotherapy, these results may provide sophisticated opportunities for the design and development of new anticancer agents.

ACKNOWLEDGEMENTS

The authors thank and acknowledge CSIR-IICT, Hyderabad and CSIR-CCMB, Hyderabad for the Funding, Scientific and Instrumental support (IICT Comm. No.: IICT/Pubs./2020/290).

REFERENCES

1. (a) Wesche J, Haglund K, Haugsten EM. Fibroblast growth factors and their receptors in cancer. Biochem J. 2011; 437: 199-213. (b) Mareel M, Leroy A. Clinical, cellular, and molecular aspects of cancer invasion. Physiol Rev. 2003; 83: 337-376.

2. (a) Vijayaraghavalu S, Peetla C, Lu S, Labhasetwar, V. Epigenetic modulation of the biophysical properties of drug-resistant cell lipids to restore drug transport and endocytic functions. Mol Pharm. 2012; 9: 2730-2742. (b) Solyanik GI. Multifactorial nature of tumor drug resistance. Exp Oncol. 2011, 32: 181-185. (c) Grant, SK. Therapeutic protein kinase inhibitors. Cell Mol Life Sci. 2009; 66: 1163-1177.

3. (a) Paul A, Bhattacharya, S. Chemistry and biology of DNA-binding small molecules. Curr Sci. 2012; 102: 212-231. (b) Meunier, B. Hybrid molecules with a dual mode of action: dream or reality? Acc Chem Res. 2012; 102:212-231.

4. Hurley, LH. DNA and its associated processes as targets for cancer therapy. Nat Rev Cancer. 2002; 2:188-200.

5. Chikamori K, Grozav AG. Kozuki T, Grabowski D, Ganapathi R, Ganapathi. MK. DNA topoisomerase II enzymes as molecular targets for cancer chemotherapy. Curr Cancer Drug Targets. 2010; 10: 758-771. (b) Wang JC. Cellular roles of DNA topoisomerases: a molecular perspective Nat. Rev Mol Cell Biol. 2002; 3: 430-440. (c) Champoux, JJ. DNA topoisomerases: structure, function, and mechanism. Annu Rev Biochem, 2001; 70: 369-413. (d) Wang, JC. DNA topoisomerases. Annu Rev Biochem. 1996; 65: 635-692.

6. Liu Y-Q, Li W-Q, Morris-Natschke SL, Qian K, Yang L, Zhu G-X, et al. Perspectives on biologically active camptothecin derivatives. Med Res Rev. 2015; 35: 753-789.

7. (a) Chen Q, Chao R, Chen H, Hou X, Yan H, Zhou S, et al. Antitumor and neurotoxic effects of novel harmine derivatives and structure-activity relationship analysis. Int J Cancer, 2005; 114: 675-682. (b) Chen Z, Cao R, Shi B, Yi W, Yu L, Song H, et al. Synthesis of novel β-carbolines with efficient DNA-binding capacity and potent cytotoxicity. Bioorg Med Chem Lett. 2010; 20: 3876-3879. (c) Sobhani AM, Ebrahimi SA, Mahmoudian M. An in vitro evaluation of human DNA topoisomerase I inhibition by Peganum harmala L. seeds extract and its beta-carboline alkaloids. J Pharm Pharm Sci. 2002; 5: 19-23.

8. (a) Cao R, Peng W, Wang Z, Xung A. β-Carboline alkaloids: biochemical and pharmacological functions. Curr Med Chem. 2007; 14: 479-500. (b) Dighe SU, Khan S, Soni I, Jain P, Shukla S, Yadav R, et al. Synthesis of β-carboline-based N- heterocyclic carbenes and their antiproliferative and antimetastatic activities against human breast cancer cells. J Med Chem. 2015; 58; 3485-3499. (c) Chen H, Gao P, Zhang M, Liao W, Zhang J. Synthesis and biological evaluation of a novel class of β- carboline derivatives. New J Chem. 2014; 38: 4155-4166. (d) Wang S, Fang K, Dong G, Chen S, Liu N, Miao Z, et al. Scaffold diversity inspired by the natural product evodiamine: Discovery of highly potent and multitargeting antitumor agents. J Med Chem. 2015; 58: 6678-6696. (e) Du H, Gu H, Li N, Wang J. Synthesis and biological evaluation of bivalent β-carbolines as potential anticancer agents. Med Chem Commun. 2016; 7: 636-645.. (f) Sorbera LA, Martin L, Leeson PA, Castaner J. Treatment of erectile dysfunction, treatment of female sexual dysfunction, phosphodiesterase 5 inhibitor. Drugs Fut. 2001; 26:15-19. (g) Daugan A, Grondin P, Ruault C, de Gouville ACLM, Coste H, Kirilovsky J, et al. The discovery of tadalafil: a novel and highly selective PDE5 inhibitor. 1: 5,6,11,11a-tetrahydro-1H-imidazo[1',5':1,6]pyrido[3,4-b]indole-1,3(2H)-dione analogues. J Med Chem. 2003; 46: 4525-4532. (h) Barnes EC, Kumar R, Davis, RA. The use of isolated natural products as scaffolds for the generation of chemically diverse screening libraries for drug discovery. Nat Prod Rep. 2016; 33: 372-381. (i) Bálint B, Wéber C, Cruzalegui F, Burbridge M, Kotschy A. Structure-based design and synthesis of harmine derivatives with different selectivity profiles in kinase versus monoamine oxidase inhibition. ChemMedChem, 2017; 12: 932-939. (j) Nagula S, Tokala R, Thatikonda S, Sana S, Vanteddu US, Godugu, C. Design and synthesis of DNA-interactive β- carboline-oxindole hybrids as cytotoxic and apoptosis-inducing agents. ChemMedChem, 2018; 13: 1009-1922.

9. (a) Cao R, Peng W, Chen H, Ma Y, Liu X, Hou X, et al. DNA binding properties of 9-substituted harmine derivatives, Biochem Biophys Res Commun. 2005; 338: 1557- 1563. (b) Song Y, Wang J, Teng SF, Kesuma D, Deng Y, Duan J, et al. Beta- carbolines as specific inhibitors of cyclin-dependent kinases. Bioorg Med Chem Lett. 2002; 12: 1129-1132. (c) Kamal A, Srinivasulu V, Nayak VL, Sathish M, Shankaraiah N, Bagul C, et al. Design and synthesis of C3-pyrazole/chalcone-linked beta-carboline hybrids: antitopoisomerase I, DNA-interactive, and apoptosis-inducing anticancer agents. ChemMedChem, 2014; 9: 2084-2098. (d) Sathish M, Dushantrao SC, Krishna NH, Nekkanti S, Tangella Y, Srinivas G, et al. Synthesis of DNA interactive C3-trans-cinnamide linked β-carboline conjugates as potential cytotoxic and DNA topoisomerase I inhibitors. Bioorg Med Chem. 2018; 26: 4916-4929. (e) Sathish M, Kavitha B, Nayak VL, Tangella Y, Ajitha A, Nekkanti S, et al. Synthesis of podophyllotoxin linked β-carboline congeners as potential anticancer agents and DNA topoisomerase II inhibitors. Eur J Med Chem. 2018; 144: 557-571

10. (a) Chen Z, Cao R, Shi B, Guo L, Sun J, Ma Q, et al. Synthesis and biological evaluation of 1,9-disubstituted β-carbolines as potent DNA intercalating and cytotoxic agents. Eur J Med Chem. 2011; 46: 5127-5137. (b) Taira Z, Kanzawas S, Dohara C, Ishida S, Matsumoto M, Sakiya, Y. Intercalation of six β-carboline derivatives into DNA. Jpn J Toxicol Environ Health, 1997; 43: 83-91.

11. (a) Bourdouxhe-Housiaux C, Colson P, Houssier C, Waring MJ, Bailly, C. Interaction of a DNA-threading netropsin-amsacrine combilexin with DNA and chromatin. Biochemistry, 1996; 35: 4251-426. (b) Nekkanti S, Pooladanda V, Veldandi M, Tokala R, Godugu C, Shankaraiah N. Synthesis of 1,2,3-Triazolo-fused-tetrahydro-β- carboline Derivatives via 1,3-Dipolar Cycloaddition Reaction: Cytotoxicity Evaluation and DNA-Binding studies. ChemistrySelect, 2017; 2: 7210-7221. (c) Barbosa VA, Formagio ASN, Savariz FC, Foglio MA, Spindol HM, Carvalho JE, et al. Synthesis and antitumor activity of β-carboline 3-(substituted-carbohydrazide) derivatives. Bioorg Med Chem. 2011; 19: 6400–6408.

12. Trujillo JI, Meyers M., Anderson DR, Hegde S, Mahoney MW, Vernier WF, et al. Novel tetrahydro-β-carboline-1-carboxylic acids as inhibitors of mitogen activated protein kinase-activated protein kinase 2 (MK-2). Bioorg Med ChemLett. 2007; 17: 4657-4663.

13. (a) Song Y, Wang J, Teng SF, Kesuma D, Deng Y, Duan J, et al. β-Carbolines as specific inhibitors of cyclin-dependent kinases. Bioorg Med Chem Lett. 2002; 12:1129-1132. (b) Song Y, Kesuma D, Wang J, Deng Y, Duan J, Wang JH, Qi RZ. pecific inhibition of cyclin-dependent kinases and cell proliferation by harmine. Biophys Res Commun. 2004; 317: 128-132. (c) Li Y, Liang F, Jiang W, Yu F, Cao R, Ma Q, et al. DH334, a β-carboline anti-cancer drug, inhibits the CDK activity of budding yeast. Cancer Biol Ther. 2007; 6: 1204-1210.

14. Barsanti PA, Wang W, Ni Z, Duhl D, Brammeier N, Martin E. The discovery of tetrahydro-beta-carbolines as inhibitors of the kinesin Eg5. Bioorg Med Chem Lett. 2010; 20:157-160.

15. Castro AC, Dang LC, Soucy F, Grenier L, Mazdiyasni H, Hottelet M, et al. Novel IKK inhibitors: beta-carbolines. Bioorg Med Chem Lett. 2003; 13: 2419-2422.

16. (a) Zhang J, Li Y, Guo L, Cao R, Zhao P, Jiang W, et al. DH166, a beta-carboline derivative, inhibits the kinase activity of PLK1. Cancer Biol Ther. 2009; 8: 2374- 2383. (b) Han X, Zhang J, Guo L, Cao R, Li Y, Li N, et al. A series of beta-carboline derivatives inhibit the kinase activity of PLKs. PLoS One, 2012; 7: e46546.

17. Ling Y, Feng J, Luo L, Guo J, Peng Y, Wang T, et al. Design and Synthesis of C3- Substituted β-Carboline-Based Histone Deacetylase Inhibitors with Potent Antitumor Activities. ChemMedChem, 2017; 12: 646-651.

18. (a) Formagio AS, Tonin LT, Foglio MA, Madjarof C, de Carvalho JE, da Costa WF, et al. Synthesis and antitumoral activity of novel 3-(2-substituted-1,3,4-oxadiazol-5- yl) and 3-(5-substituted-1,2,4-triazol-3-yl) β-carboline derivatives. Bioorg Med Chem. 2008; 16: 9660-9667. (b) Savariz F, Foglio MA, de Carvalho JE, Ruiz AL, Duarte MC, da Rosa MF, et al. Synthesis and evaluation of new β-carboline-3-(4- benzylidene)-4H-oxazol-5-one derivatives as antitumor agents. Molecules, 2012; 17: 6100-6113. (c) Barbosa VA, Formagio AS, Savariz FC, Foglio MA, Spindola H, de Carvalho JE, et al. Synthesis and antitumor activity of β-carboline 3-(substituted-carbohydrazide) derivatives. Bioorg Med Chem. 2011; 19: 6400-6408.

19. (a) Inokuma T, Furukawa M, Uno T, Suzuki Y, Yoshida K, Yano Y, et al. Bifunctional hydrogen-bond donors that bear a quinazoline or benzothiadiazine skeleton for asymmetric organocatalysis. Chem –Eur J. 2011; 17: 10470-10477. (b) Shakhidoyatov KM, Elmuradov BZ. Tricyclic Quinazoline Alkaloids: Isolation, Synthesis, chemical modification, and biological activity. Chem Nat Compd. 2014; 5: 781-800. (c) Ji-Feng L. Rapid syntheses of biologically active quinazolinone natural products using microwave technology. Curr Org Synth. 2007; 4: 223–237.

20. (a) Pao W, Miller V, Zakowski M. EGF receptor gene mutations are common in lung cancers from "never smokers" and are associated with sensitivity of tumors to gefitinib and erlotinib. Proc Natl Acad Sci U.S.A, 2004; 101: 13306-13311. (b) Raymond E, Faivre S, Armand J. Epidermal growth factor receptor tyrosine kinase as a target for anticancer therapy. Drugs, 2000; 60: 15-23.

21. (a) Mathew T, Papp AA, Paknia F, Fustero S, Prakash GKS. Benzodiazines: recent synthetic advances. Chem Soc Rev. 2017; 46: 3060-3094. (b) Kshirsagar UA. Recent . (c) Khan I, Ibrar A, Abbas N, Saeed A. Recent advances in the structural library of functionalized quinazoline and quinazolinone scaffolds: Synthetic approaches and multifarious applications. Eur J Med Chem. 2014; 76: 193-244. (d) Witt A, Bergman J. Recent developments in the field of quinazoline chemistry. Curr Org Chem, 2003; 7: 659-677.

22. (a) Jafari E, Khajouei MR, Hassanzadeh F, Hakimelahi GH, Khodarahmi, GA. Quinazolinone and quinazoline derivatives: recent structures with potent antimicrobial and cytotoxic activities. Res Pharm Sci. 2016; 11: 1-14. (b) Chen K, Wang K, Kirichian AM, Al Aowad AF, Iyer LK, Adelstein SJ, Kassis AI. In silico design, synthesis, and biological evaluation of radioiodinated quinazolinone derivatives for alkaline phosphatase–mediated cancer diagnosis and therapy. Mol Cancer Ther. 2006; 5: 3001-3013. (c) Pomarnacka E, Maruszak M, Langowska K, Reszka P, Bednarski PJ. Synthesis and cytotoxicity testing of novel 2-(3-substituted-6-chloro-1,1-dioxo-1,4,2-benzodithiazin-7-yl)-3-phenyl-4(3H)-quina zolinones. Arch Pharm Chem Life Sci. 2008; 341: 485–490.

23. (a) Garofalo A, Goossens L, Baldeyrou B, Lemoine A, Ravez S, Six P, et al. Design, synthesis, and DNA-binding of N-alkyl(anilino)quinazoline derivatives. J Med Chem. 2010; 53: 8089-8103. (b) Sinha S, Srivastava M. Biologically active quinazolines. Prog Drug Res. 1994; 4: 143–238. (c) Liverton NJ, Armstrong DJ, Claremon DA, Remy DC, Baldwin JJ, Lynch RJ, et al. Nonpeptide glycoprotein IIb/IIIa inhibitors: substituted quinazolinediones and quinazolinones as potent fibrinogen receptor antagonists. Bioorg Med Chem Lett. 1998; 8: 483–486.

24. Griffin RJ, Srinivasan S, Bowman K, Calvert AH, Curtin NJ, Newell DR, et al. Resistance-Modifying Agents. 5. Synthesis and biological properties of quinazolinone inhibitors of the DNA repair enzyme poly(ADP-ribose) polymerase (PARP). J Med Chem. 1998; 41: 5247-5256.

25. (a) Jiao RH, Xu S, Liu JY, Ge HM, Ding H, Xu C, et al. Chaetominine, a cytotoxic alkaloid produced by endophytic chaetomium sp. IFB-E015. Org Lett. 2006; 8: 5709- 5712. (b) Hour M-J, Yang J-S, Lien J-C, Kuo S-C, Huang L-J. Synthesis and Cytotoxicity of 6-pyrrolidinyl-2-(2-substituted phenyl)-4-quinazolinones. J Chin Chem Soc. 2007; 54: 785-790.

26. (a) Dancey JE, Chen HX. Strategies for optimizing combinations of molecularly targeted anticancer agents. Nat Rev Drug Discovery, 2006; 5: 649-659. (b) Anighoro A, Bajorath J, Rastelli G. Polypharmacology: challenges and opportunities in drug discovery. J Med Chem. 2014; 57: 7874-7887. (c) Boran AD, Iyengar R. Systems approaches to polypharmacology and drug discovery. Drug Discovery Dev. 2010; 13: 297-309.

27. (a) Vizirianakis IS, Chatzopoulou M, Bonovolias ID, Nicolaou IV, Demopoulos VJ, Tsiftsoglou, AS. Toward the development of innovative bifunctional agents to induce differentiation and to promote apoptosis in leukemia: Clinical candidates and perspectives. J Med Chem. 2010; 53: 6779-6810. (b) Avner BS, Fialho AM, Chakrabarty, AM. Overcoming drug resistance in multi-drug resistant cancers and microorganisms. Bioengineered, 2012; 3: 262-270.

28. (a) Long EC, Barton JK. On demonstrating DNA intercalation. Acc. Chem. Res. 1990; 23: 271-273. (b) Satyanarayana S, Dabrowiak JC, Chaires JB. Tris(phenanthroline)ruthenium(II) enantiomer interactions with DNA: mode and specificity of binding. Biochemistry, 1993; 32: 2573-2584.

29. Pommier Y, Pourquier P, Fan Y, Strumberg D. Mechanism of action of eukaryotic DNA topoisomerase I and drugs targeted to the enzyme. Biochim Biophys Acta, 1998; 1400: 83-105. (b) Bailly C. Topoisomerase I poisons and suppressors as anticancer drugs. Curr Med Chem, 2000; 7; 39-58.

30. Eng WK, Faucette L, Johnson RK, Sternglanz R. Evidence that DNA topoisomerase I is necessary for the cytotoxic effects of camptothecin. Mol Pharmacol. 1988; 34: 755- 760.

31. Nitiss J, Wang JC. DNA topoisomerase-targeting antitumor drugs can be studied in yeast. Proc Natl Acad Sci U S A 1988; 85: 7501- 7505.

32. Leteurtre F, Fesen M, Kohlhagen G, Kohn K, Pommier Y. Specific interaction of camptothecin, a topoisomerase I inhibitor, with guanine residues of DNA detected by photoactivation at 365 nm. Biochemistry, 1993; 32: 8955-8962.

33. Barton JK, Dennenberg JJ, Kumar CV, Turro, NJ. Binding modes and base specificity of tris(phenanthroline)ruthenium(II) enantiomers with nucleic acids: Tuning the stereoselectivity. J Am Chem Soc. 1986; 108: 2081-2088.

34. (a) Gonzalez MM, Vignoni M, Magali PM, Ales-Gandolfo MA, Gonzalez-Baro MR, Rosa EB, et al. Photosensitization of DNA by β-carbolines: Kinetic analysis and photoproduct characterization. Org Biomol Chem. 2012; 10: 1807-1819. (b) Vignoni M, Rasse-Suriani FAO, Butzbach K, Erra-Balsells R, Epe B, Cabrerizo FM. Mechanisms of DNA damage by photoexcited 9-methyl-β-carbolines. Org Biomol Chem. 2013; 11: 5300-5309. (c) David-Cordonnier MH, Hildebrand MP, Baldeyrou B, Lansiaux A, Keuser C, Benzschawel K, Lemster T, Pindur U. Design, synthesis and biological evaluation of new oligopyrrole carboxamides linked with tricyclic DNA-intercalators as potential DNA ligands or topoisomerase inhibitors. Eur J Med Chem. 2007; 42: 752-771. (d) Foxon SP, Phillips T, Gill MR, Towrie M, Parker AW, Webb M, Thomas JA. Multifunctional light switch: DNA binding and cleavage properties of a heterobimetallic ruthenium–dhenium dipyridophenazine complex. Angew Chem, Int Ed. 2007; 46: 3686-3688.

35. Lakowicz J. in: Principles of Fluorescence Spectroscopy. second ed., Plenum, New York, 1999. (b) Wu J, Zhao M, Qian K, Lee K-H, Morris-Natschke S, Peng S. Novel N-(3-carboxyl-9-benzyl-beta-carboline-1-yl)ethylamino acids: synthesis, anti- tumor evaluation, intercalating determination, 3D QSAR analysis and docking investigation Eur J Med Chem. 2009; 44: 4153- 4161.

36. Nyarko E, Hanada N, Habib A, Tabata M. Fluorescence and phosphorescence spectra of Au(III), Pt(II) and Pd(II) porphyrins with DNA at room temperature. Inorg Chim Acta, 2004; 357: 739-745.

37. Jiang X, Shang L, Wang ZX, Dong S. Spectrometric and voltammetric investigation of interaction of neutral red with calf thymus DNA: pH effect. J Biophy Chem. 2005; 118: 42-50.

38. Fukuda H, Katahira M, Tsuchiya N, Enokizono Y, Sugimura T, Nagao M, Nakagama H. Unfolding of quadruplex structure in the G-rich strand of the minisatellite repeat by the binding protein UP1. PNAS USA, 2002; 99; 12685-12690.

39. Suh D, Chaires JB. Criteria for the mode of binding of DNA binding agents. Bioorg Med Chem. 1995; 3: 723-728. (b) Butour JL, Macquet JP. Viscosity, nicking, thermal and alkaline denaturation studies on three classes of DNA-platinum complex. Biophys Acta Nucleic Acids Protein Synth. 198; 653: 305-315. (c) Arjmand F, Parveen S, Afzal M, Shahid M. Synthesis, characterization, biological studies (DNA binding, cleavage, antibacterial and topoisomerase I) and molecular docking of copper(II) benzimidazole complexes. J Photochem Photobiol B, 2012; 114: 15-26. (d) Topala T, Bodoki A, Oprean L, Oprean R. Experimental techniques employed in the study of metal complexes-DNA–interactions. Farmacia, 2014; 62: 1049-1060.

40. Botta M, Armaroli S, Castagnolo D, Fontana G, Perad P, Bombardelli E. Synthesis and biological evaluation of new taxoids derived from 2-deacetoxytaxinine. Bioorg Med Chem Lett. 2007; 17: 1579-1583.

41. Szumilak M, Szulawska–Mroczek A, Koprowska K, Stasiak M, Lewgowd W, Stanczak A, Czyz M. Synthesis and in vitro biological evaluation of new polyamine conjugates as potential anticancer drugs. Eur J Med Chem. 2010; 45: 5744-5751.

42. Dexheimer TS, Pommier Y. DNA cleavage assay for the identification of topoisomerase I inhibitors. Nat Protoc, 2008; 3: 1736-1750.

43. Tan CP, Liu J, Chen LM, Shi S, Ji LN. Synthesis, structural characteristics, DNA binding properties and cytotoxicity studies of a series of Ru(III) complexes. J Inorg Biochem. 2008; 102: 1644-1653.

44. Staker BL, Feese MD, Cushman M, Pommier Y, Zembower D, Stewart L, Burgin AB. Structures of three classes of anticancer agents bound to the human topoisomerase I–DNA covalent complex. J Med Chem, 2005; 48: 2336-2345.

Cite this article

Tangella Y, Sathish M, Kadagathur M, Nagesh N, Babu BN (2021) Design, Synthesis and Biological Evaluation of Hybrid C3-Quinazolinone linked β-carboline Conjugates as DNA Intercalative Topoisomerase I Inhibitors. J Clin Pharm 5(1): 1020.